

# **An inactivated multivalent influenza A virus vaccine is broadly protective in mice and ferrets**

Jaekeun Park<sup>1</sup>, Sharon Fong<sup>1</sup>, Louis M. Schwartzman<sup>1#</sup>, Zhong-Mei Sheng<sup>1</sup>, Ashley Freeman<sup>1</sup>, Lex Matthews<sup>1</sup>, Yongli Xiao<sup>1</sup>, Mitchell D. Ramuta<sup>1,\$</sup>, Natalia A. Batchenkova<sup>1,@</sup>, Li Qi<sup>1</sup>, Luz Angela Rosas<sup>1</sup>, Stephanie Williams<sup>1</sup>, Kelsey Scherler<sup>2</sup>, Monica Gouzoulis<sup>3</sup>, Ian Bellay<sup>4</sup>, David M. Morens<sup>5</sup>, Kathie-Anne Walters<sup>2</sup>, Matthew J. Memoli<sup>3</sup>, John C. Kash<sup>1</sup>, Jeffery K. Taubenberger<sup>1,\*</sup>

<sup>1</sup>Viral Pathogenesis and Evolution Section, Laboratory of Infectious Diseases, National Institute of Allergy and Infectious Diseases, National Institutes of Health, Bethesda, MD 20892 USA

<sup>2</sup>Institute for Systems Biology, Seattle, WA 98109 USA

<sup>3</sup>Clinical Studies Unit, Laboratory of Infectious Diseases, National Institute of Allergy and Infectious Diseases, National Institutes of Health, Bethesda, MD 20892 USA

<sup>4</sup>Laboratory of Infectious Diseases, National Institute of Allergy and Infectious Diseases, National Institutes of Health, Bethesda, MD 20892 USA

<sup>5</sup>Office of the Director, National Institute of Allergy and Infectious Diseases, National Institutes of Health, Bethesda, MD 20892 USA

\*Corresponding Author. Email: [taubenbergerj@niaid.nih.gov](mailto:taubenbergerj@niaid.nih.gov)

#Current address: Safety and Operations Support Branch, Office of the Director, National Institutes of Health Bethesda, MD 20892 USA

\$Current address: Pathology & Laboratory Medicine Department, University of Wisconsin, Madison, WI, 53711 USA

25 @Current address: College of Medicine, University of Nebraska Medical Center, Omaha, NE  
26 68198 USA  
27

28 **Keywords**

29 Influenza A virus, universal influenza vaccine, correlates of protection, pathology, heterosubtypic  
30 immunity, cellular immunity, inactivated viral vaccine, genomics

31

32 **Abstract**

33 Influenza A viruses (IAVs) present major public health threats from annual seasonal epidemics,  
34 from pandemics caused by novel virus subtypes, and from viruses adapted to a variety of animals  
35 including poultry, pigs and horses. Vaccines that broadly protect against all such IAVs, so-called  
36 “universal” influenza vaccines, do not currently exist, but are urgently needed. This study  
37 demonstrates that an inactivated, multivalent whole virus vaccine, delivered intramuscularly or  
38 intranasally, is broadly protective against challenges with multiple IAV HA/NA subtypes in both  
39 mice and ferrets, including challenges with IAV subtypes not contained in the vaccine. This  
40 vaccine approach indicates the feasibility of eliciting broad “universal” IAV protection, and  
41 identifies a promising candidate for influenza vaccine clinical development.

42

43 **One-Sentence Summary**

44 An inactivated, whole avian influenza virus vaccine delivered intramuscularly or intranasally  
45 provides extremely broad protection against antigenically divergent viral challenge and is a  
46 promising candidate for a “universal” influenza virus vaccine.

47

## 48 **Introduction**

49 Influenza A viruses (IAVs) pose a continual major public health threat. Globally, endemic (annual,  
50 or ‘seasonal’) influenza results in 3-5 million severe illnesses and up to 650,000 deaths each year  
51 (1). Influenza pandemics, in which novel IAVs unpredictably emerge from the IAV reservoir of  
52 wild waterfowl (2), and against which most humans lack protective immunity, can have even larger  
53 global impacts (3): e.g., the 1918 influenza pandemic resulted in at least 50 million deaths (4). In  
54 addition, IAVs adapted to non-human hosts emerge sporadically to infect and kill humans (e.g.,  
55 poultry-associated H5N1 and H7N9) or even pandemically (e.g., pandemic H1N1 “swine”  
56 influenza in 2009). The fact that IAVs are permanently adapted to, or repeatedly infect, a wide  
57 variety of non-human hosts such as horses, dogs, seals, and other hosts indicates that IAV risks to  
58 humans are widely distributed in nature; moreover, these viruses are comprised of a broad array  
59 of different genotypes of variable and often unpredictable human pathogenicity. Currently, the  
60 only IAV vaccines licensed for human use are made each year to match specific circulating  
61 influenza virus strains in both Northern and Southern Hemispheres (5). Such vaccines do not  
62 protect against antigenically variant annual IAV strains, new pandemic viruses, poultry-associated  
63 viruses, or viruses adapted to, or frequently infecting, other mammalian hosts. There is a critical  
64 need for influenza vaccines that broadly protect against all such IAVs, a so-called “universal”  
65 vaccine (6, 7).

66

67 IAVs are enveloped, negative-sense, single-stranded RNA viruses with 8 genome segments (8). In  
68 addition to humans, IAVs infect large numbers of warm-blooded animal hosts, including over 100  
69 avian species and many mammals (9, 10). IAVs express two major surface glycoproteins—HA  
70 and NA, and are subtyped by antigenic characterization of the HA and NA glycoproteins. Sixteen

71 HA and 9 NA subtypes are consistently found in avian hosts in various combinations (e.g.,  
72 A/H1N1 or A/H3N2), and these wild bird viruses are thought to be the ultimate source of human  
73 pandemic influenza viruses (9). IAV genome segmentation allows for viral reassortment, and since  
74 HA and NA are encoded on separate gene segments, novel IAVs of any of the 144 possible subtype  
75 combinations can theoretically be generated following mixed infections in a host, in a process  
76 called “antigenic shift”. IAVs are also evolutionarily dynamic RNA viruses with high mutation  
77 rates. Mutations that change amino acids in the antigenic portions of HA and NA proteins may  
78 allow human-adapted strains to evade population immunity, a process termed “antigenic drift”.  
79 Despite enhanced surveillance, future pandemics cannot yet be predicted, including when and  
80 where a pandemic virus strain will emerge, what the viral subtype will be, how pathogenic it will  
81 be in humans, or whether there will be some immunologic cross-reactivity with prior circulating  
82 IAVs. Severe human zoonotic infections with poultry-origin IAVs have also been observed,  
83 including recent human infections with A/H5N1 and A/H7N9 viruses (11).

84  
85 An effective ‘universal’ vaccine would ideally provide broad protection against all IAV subtypes  
86 found in birds, domestic mammals, and humans. Efforts to develop such broadly protective  
87 vaccines have been under way for decades (12) and have included experimental vaccines  
88 specifically targeting the M2 ectodomain (13, 14) or NA (15, 16) proteins to stimulate the  
89 development of protective antibody responses, vaccines based on antigens that stimulate  
90 development of T-cell responses (17), and most recently, a variety of vaccine approaches targeting  
91 antigenically conserved epitopes on the HA head and stalk (18-21). However, a practical vaccine  
92 inducing broad heterosubtypic or universal protection has not been previously demonstrated with  
93 any of the above approaches.

94

95 In the present study, mice and ferrets vaccinated with a whole-virus beta-propiolactone (BPL)  
96 inactivated vaccine cocktail intranasally or intramuscularly were subsequently challenged with  
97 multiple IAVs. Challenge viruses included homosubtypic viruses (strains with antigenically  
98 variable HA and NA subtypes sharing vaccine virus subtypes, as examples of protection against  
99 annual influenza) and heterosubtypic viruses (strains with HA and/or NA subtypes not present in  
100 the vaccine, as examples of zoonotic and pandemic IAVs) viruses showed near 100% protection.  
101 The vaccine cocktail included four inactivated wild-type, low pathogenicity avian influenza  
102 viruses: H1N9, H3N8, H5N1, and H7N3. The four HA subtypes were chosen to reflect the  
103 subtypes of currently circulating annual IAV strains (H1 and H3) or recent epizootic IAV  
104 infections (H5 and H7) and represent both major phylogenetic HA groupings—clade 1 (H1 and  
105 H5) and clade 2 (H3 and H7) (20), along with four different NA subtypes representing the two  
106 major NA clades (2).

107

## 108 **Results**

109 **Immune responses to IM and IN vaccination in mice and protection against homosubtypic**  
110 **and heterosubtypic viral challenge.** The multivalent vaccine was prepared using BPL-  
111 inactivation of avian IAV H1N9, H3N8, H5N1, and H7N3 subtypes, grown in Madin-Darby  
112 Canine Kidney (MDCK) cells, and purified by sucrose density gradient. Mice were primed on day  
113 0 and boosted 28 days later by intramuscular (IM) or intranasal (IN) vaccination with 6ug total  
114 protein (1.5ug per subtype). An overview of animal studies is depicted in Supplementary Fig. S1.  
115 The vaccine was highly immunogenic in mice and both IN and IM immunization elicited  
116 significant serum IgG antibody responses to homologous HAs (H1, H3, H5, H7) and NAs (N1,

117 N3, N8, N9) as well as hemagglutination inhibition (HAI) antibodies (Fig. 1A,B, Supplementary  
118 Fig. S2A). Although IM immunization induced generally higher serum IgG antibody responses  
119 than IN immunization (Fig 1A,B), IN immunization induced a more pronounced IgA response in  
120 bronchoalveolar lavage (BAL) fluid (Supplementary Fig. S2B,C). Additionally, antibodies to the  
121 conserved stalk (or stem) regions of both group 1 and group 2 HAs were generated by IM or IN  
122 immunization (Supplementary Fig. S2D,E).

123

124 To evaluate vaccine efficacy against viral challenge, cohorts of BPL-inactivated vaccinated  
125 animals were challenged with six IAV strains at a 10x mouse LD<sub>50</sub> dose (Supplementary Table 2).  
126 Mock-vaccinated animals steadily lost weight and showed 100% mortality following challenge  
127 with each of these viruses (Fig. 1C-H). IM and IN vaccination provided 100% protection against  
128 lethal 10x LD<sub>50</sub> challenge with the fully reconstructed 1918 pandemic H1N1 and zoonotic H7N9  
129 viruses (Fig. 1C,D) with little associated weight loss. Lethal 10x LD<sub>50</sub> challenge with a highly  
130 pathogenic avian influenza (HPAI) H5N8 virus (Fig. 1E) showed 90% protective efficacy for this  
131 antigenically variant, systemically replicating HPAI virus following IM vaccination. Protective  
132 efficacy of IN vaccination against this HPAI virus was less than that observed for IM vaccination,  
133 with 70% survival following lethal H5N8 challenge.

134

135 To study the effects of vaccination following lethal challenge with homosubtypic, partially  
136 heterosubtypic (challenge with a virus with a novel HA subtype) and completely heterosubtypic  
137 (challenge with a virus with a novel HA and NA subtype), immunized mice were challenged with  
138 chimeric avian H7N1, H6N1, and H10N7 (20, 22), respectively. These viruses were chosen to  
139 represent different antigenic distance from the vaccine antigens (Supplementary Table 2). The

140 H7N1 virus HA matched the vaccine H7 HA, along with a minor mismatch in N1. In contrast, the  
141 H6N1 challenge used the same NA as in the H7N1 challenge but in this case with an HA subtype  
142 not contained in the vaccine. The H10N7 virus expressed both HA and NA subtypes not contained  
143 in the vaccine. In all three challenge experiments, both IM- and IN-vaccinated mice showed 100%  
144 survival.

145  
146 Vaccinated and PBS-vaccinated (mock) mice were challenged with a 10x LD<sub>50</sub> dose of the H7N1  
147 subtype virus. Vaccinated mice lost very little weight and all survived lethal challenge, in contrast  
148 to mock-vaccinated mice, which showed a rapid decline in body weight with 100% fatality  
149 occurring between days 6-8 post-challenge (Fig. 1F). A second cohort of vaccinated and mock-  
150 vaccinated mice were challenged with a 10x LD<sub>50</sub> dose of the H6N1 virus. Vaccinated mice lost  
151 less weight and had 100% survival following lethal challenge, in contrast to mock-vaccinated,  
152 challenged mice, which showed a rapid decline in body weight and 100% fatality by days 6-7 post-  
153 challenge (Fig. 1G). Interestingly, IM vaccinated mice showed more early weight loss than IN  
154 vaccinated mice, with weight loss on days 1-4 weight loss similar to mock vaccinated groups, but  
155 with recovery and 100% survival. In a third cohort, mice were challenged with a 10x LD<sub>50</sub> dose  
156 of the H10N7 virus to examine protection of vaccination against completely heterosubtypic viral  
157 infection. Both IM and IN vaccinated mice lost significantly less weight through day 4, but then  
158 rapidly recovered and had 100% survival following lethal challenge, in contrast to mock  
159 vaccinated challenged mice, which showed a steady decline in body weight and 100% fatality by  
160 days 6-7 post-challenge (Fig. 1H). Together, these results showed that vaccination of mice resulted  
161 in broad protection from a variety of lethal challenges with viruses of varying degrees of HA and  
162 NA antigenic distances. In five of the six different lethal viral challenge experiments, both IM and



163 IN mice showed 100% survival, with 0% survival of mock-vaccinated animals. For HPAI H5N8  
164 challenge, IM and IN vaccination afforded 90% and 70% protection, respectively.

165

166 **Pulmonary gene expression responses during mismatched and heterosubtypic challenge in**

167 **mice.** To determine the effects of vaccination on pulmonary inflammatory and immune responses

168 during viral infection, expression microarray analysis was performed on lung tissue collected from

169 mock and vaccinated animals on day 6 following challenge with chimeric H7N1, H6N1, and

170 H10N7 chimeric viruses. Viral replication in whole lung tissue measured by qPCR did not detect

171 M gene viral RNA by 3 to 6 days post-challenge with H7N1 and H6N1 viruses, and showed nearly

172 90% reduction in viral RNA by 6 days post-H10N7 challenge (Fig. 2A). Analysis of variance

173 (ANOVA) identified significantly differentially expressed genes ( $\geq 2$ -fold difference in median

174 expression,  $p < 0.05$ ) between mock, IN and IM challenged animals. Expression levels of genes

175 associated with type I interferon (IFN) responses, lymphocyte activation, reactive oxygen species

176 responses and DNA damage, and programmed cell death were significantly reduced in IN and IM

177 vaccinated mice challenged with H7N1, H6N1, and H10N7 compared to PBS-vaccinated,

178 challenged animals (Fig. 2A). Higher expression levels of these genes in PBS-vaccinated animals

179 correlated with higher viral replication levels. Concordant with the weight loss in vaccinated

180 animals observed following completely heterosubtypic H10N7 lethal challenge compared to either

181 H7N1 and H6N1, IN- and IM-vaccinated animals showed slightly stronger immune-response

182 related gene expression in response to H10H7 (Fig. 2A). These animals also showed slightly higher

183 levels of viral replication.

184

185 IN vaccinated animals showed more robust gene expression responses compared to IM vaccinated  
186 mice; direct comparison (t test, 2-fold difference in median expression, p value <0.05) of IN- and  
187 IM-vaccinated animals revealed subtle but significant differences in gene expression  
188 (Supplementary Fig. S3A) that showed enrichment of pathways for neutrophil adhesion, IFN  
189 signaling, cytokine/chemokine signaling, dendritic cell maturation and other pathways involved in  
190 innate response to infection (Supplementary Fig. S3B).

191

192 **Lung pathology and immune cell infiltrates during mismatched and heterosubtypic**  
193 **challenge in mice.** Histopathological examination was performed on mouse lung sections at day  
194 5 post-viral challenge (Fig. 2B and Supplementary Fig. S4-6) for H7N1, H6N1, and H10N7  
195 experiments.

196

197 Lung sections of mock-vaccinated mice challenged with H7N1 showed marked pathological  
198 changes involving over 50% of the lung parenchyma, including multifocal, moderate-to-severe,  
199 necrotizing bronchitis and bronchiolitis, along with moderate-to-severe alveolitis with pulmonary  
200 edema and fibrinous exudates (Fig. 2B and Supplementary Fig 5). Influenza viral antigen staining  
201 showed widespread positivity in respiratory epithelial cells and in alveolar epithelial cells. In  
202 contrast, lung sections from IM- and IN-vaccinated animals challenged with H7N1 (both HA and  
203 NA represented in the vaccine) showed minimal histopathological changes, an absence of  
204 alveolitis and no viral antigen in alveolar epithelial cells. The respiratory epithelium of bronchi  
205 and bronchioles was intact. Sections from mock-vaccinated mouse lungs showed occasional  
206 CD19+ B cells and CD3+ T lymphocytes, but abundant Ly6G+ neutrophils throughout the lung  
207 parenchyma. In contrast, IM- and IN-vaccinated mouse lungs showed increased CD19+ and CD3+

208 lymphocyte aggregates especially prominent in perivascular and peribronchiolar locations and a  
209 marked reduction in lung parenchymal neutrophils. Large aggregates of CD19- plasma cells were  
210 observed focally in the lungs of vaccinated mice.

211  
212 Similarly, lung sections of mock-vaccinated mice challenged with H6N1 showed marked  
213 pathological changes involving over 50% of the lung parenchyma, including multifocal, moderate-  
214 to-severe, necrotizing bronchitis and bronchiolitis, along with moderate-to-severe alveolitis with  
215 pulmonary edema and fibrinous exudates (Fig. 2B and Supplementary Fig S5). Influenza viral  
216 antigen staining showed widespread positivity in respiratory epithelial cells and in alveolar  
217 epithelial cells. In contrast, lung sections, from IM- and IN-vaccinated animals challenged with  
218 the partially heterosubtypic H6N1 virus, showed minimal histopathological changes, and rapidly  
219 reepithelializing respiratory epithelium in bronchi and bronchioles characterized by abundant  
220 mitotic figures, an absence of alveolitis and no viral antigen in alveolar epithelial cells. Sections  
221 from mock-vaccinated mouse lungs showed occasional CD19+ B cells, CD3+ T cells, and  
222 abundant Ly6G+ neutrophils throughout the lung parenchyma, with prominent parenchymal  
223 neutrophil infiltrates and neutrophil margination from pulmonary blood vessels. In contrast, IM-  
224 and IN-vaccinated mouse lungs showed markedly increased CD19+ B and CD3+ T lymphocyte  
225 aggregates, especially in perivascular and peribronchiolar locations and a marked reduction in lung  
226 parenchymal neutrophils. Lung sections from vaccinated mice showed foci of bronchiolar intra-  
227 epithelial CD19+ B cells, and multifocal accumulations of CD-19- plasma cells in peribronchiolar  
228 and perivascular locations. These results demonstrated that both IM and IN vaccination in mice  
229 resulted in complete protection from lethal challenge with a partially heterosubtypic lethal H6N1  
230 viral challenge, associated with dramatic reductions in viral titer, pathologic changes, and host

231 immune and inflammatory responses in lung, and a marked increase in B and T cell aggregates in  
232 the lungs of vaccinated mice.

233

234 Lung sections of mock-vaccinated mice challenged with H10N7 showed marked pathological  
235 changes involving over 50% of the lung parenchyma, including multifocal, moderate-to-severe,  
236 necrotizing bronchitis and bronchiolitis, along with moderate-to-severe alveolitis with a  
237 neutrophil-predominant, mixed cellularity inflammatory infiltrate, pulmonary edema and fibrinous  
238 exudates (Fig. 2B and Supplementary Fig S6). Influenza viral antigen staining showed widespread  
239 positivity in respiratory epithelial cells and in alveolar epithelial cells. In contrast, lung sections,  
240 from IM- and IN-vaccinated animals challenged with the completely heterosubtypic H10N7 virus,  
241 showed a marked reduction in histopathological changes, rapidly reepithelializing respiratory  
242 epithelium in bronchi and bronchioles characterized by abundant mitotic figures, little-to-no  
243 alveolitis with little viral antigen in alveolar epithelial cells but viral antigen detected in alveolar  
244 macrophages multifocally. Sections from mock-vaccinated mouse lungs showed occasional  
245 CD19<sup>+</sup> B and CD3<sup>+</sup> T lymphocytes, and large infiltrates of Ly6G<sup>+</sup> neutrophils throughout the  
246 lung parenchyma with prominent neutrophil margination from pulmonary blood vessels. In  
247 contrast, IM- and IN-vaccinated mouse lungs showed markedly increased CD19<sup>+</sup> and CD3<sup>+</sup>  
248 lymphocyte aggregates, especially in perivascular and peribronchiolar locations and a marked  
249 reduction in lung parenchymal neutrophils. These results demonstrated that both IM and IN  
250 vaccination in mice resulted in complete protection from lethal challenge with a completely  
251 heterosubtypic H10N7 virus that was associated with dramatic reductions in viral titer, pathologic  
252 changes, and host immune and inflammatory responses in lung.

253

254 Immunization with lower doses (1/4 antigen) of the same vaccine provided 100% protection  
255 against 10x LD<sub>50</sub> lethal challenge with completely heterosubtypic H10N7 and partially  
256 heterosubtypic H6N1 viruses in mice (Supplementary Fig S7), suggesting that a lower dose of the  
257 vaccine could still provide a high level of protection. Passive serum transfer experiments in mice,  
258 in which serum from vaccinated animals was injected intraperitoneally 1 day prior to challenge in  
259 unvaccinated mice with intrasubtypic H7N1, provided 100% protection with serum from IM-  
260 vaccinated, but not from IN-vaccinated animals (Supplementary Fig. S8A), consistent with the  
261 lower levels of serum anti-viral antibody observed in IN-vaccinated animals (Fig. 1A-B). Serum  
262 transfer experiments followed by H6N1 challenge, in which the HA subtype was not contained in  
263 the vaccine, while the N1 NA subtype was, produced analogous results to intrasubtypic H7N1  
264 challenge, in that serum from IM-vaccinated mice saved unvaccinated H6N1-challenged while  
265 serum from IN-vaccinated mice did not (Supplementary Fig. S8B). In this case, protection was  
266 likely afforded by anti-neuraminidase antibody in vaccinated serum, and/or anti-group 1 HA stalk  
267 antibody. In contrast, passive serum transfer from either IM- or IN-immunized mice provided no  
268 protection against heterosubtypic H10N7 challenge in unvaccinated mice (Supplementary Fig.  
269 S8C), suggesting strongly that the complete heterosubtypic protection observed (Fig. 1H and  
270 Supplementary Fig. S6) is not primarily mediated by serum antibodies, but is likely mediated by  
271 cellular immune responses. Having demonstrated broad protective immunity in vaccinated mice  
272 following a variety of lethal challenge experiments including challenge with completely  
273 heterosubtypic viruses, the effects of vaccination against mismatched and heterosubtypic IAV viral  
274 challenge was next evaluated in ferrets.  
275

276 **Immune responses to IM and IN vaccination in ferrets and protection against mismatched**  
277 **and heterosubtypic viral challenge.** Ferrets were primed and boosted 28 days later by IM and  
278 IN vaccination with 400ug total protein (100 ug per subtype). IN vaccination was performed  
279 without adjuvant, and IM immunization was performed using a squalene-based adjuvant  
280 (Supplementary Fig. S1B). Mock-immunized control animals were intranasally inoculated with  
281 PBS or intramuscularly inoculated with PBS including adjuvant. The sequence similarities  
282 between the vaccine strains and the challenge strains are summarized in Supplementary Table 2.  
283 As shown in Fig. 3A,B, the vaccine was highly immunogenic in ferrets and both IN and IM  
284 immunization elicited significant serum IgG antibody responses to homologous HAs (H1, H3, H5,  
285 H7) and NAs (N1, N3, N8, N9) as well as serum group-1 and group-2 HA stalk antibodies and  
286 hemagglutination inhibition (HAI) antibodies (Supplementary Fig. S9A,B). Similar to what was  
287 observed in mice, IM immunization induced generally higher serum IgG antibody responses than  
288 IN immunization in ferrets (Fig. 3A,B).

289  
290 The effect of vaccination on homosubtypic A/H1N1 viral challenge in ferrets was next evaluated.  
291 Adult female ferrets were primed and boosted as above with the tetravalent, whole virus BPL-  
292 inactivated vaccine. Vaccine efficacy was evaluated following mismatched, intrasubtypic  
293 challenge with A/swine/1931 H1N1 virus (Supplementary Table 2). HAI assay demonstrated a  
294 statistically significant, approximately 4-fold difference in HAI titers between the vaccine H1 HA  
295 and the challenge H1 viruses (Supplementary Fig. S10A). The N1 NA shared only 85.5%  
296 nucleotide identity with the N1 NA in the vaccine, demonstrating that the challenge virus has  
297 substantial antigenic difference compared to vaccine antigens. Viral titers in ferret nasal wash in  
298 IM- and IN-vaccinated ferrets were significantly reduced to near undetectable levels by day 5 post-

299 challenge as compared to mock-vaccinated ferrets (Fig. 3C), and lung titers collected from IM-  
300 and IN-vaccinated ferrets at day 4 post-challenge showed no detectable levels of viral replication.

301  
302 Similarly, vaccinated and mock-vaccinated ferrets were challenged with a partially heterosubtypic  
303 human seasonal IAV, A/Port Chalmers/1973 (H3N2) (Supplementary Table 2). In this case, the  
304 H3 was antigenically mismatched to the avian H3 HA in the vaccine, as supported by cross-HAI  
305 evaluation (Supplementary Fig. S10B) and sequence identity to the vaccine H3 HA (83.8%), while  
306 the challenge virus expressed an N2 subtype NA not contained in the vaccine. The closest vaccine  
307 NA sequence shared only 43.5% identity with the challenge virus N2 subtype. Post-challenge  
308 viral titers in nasal wash in IM- and IN-vaccinated ferrets were significantly reduced to near  
309 undetectable levels by day 5 post-challenge (Fig. 3D), and lung titers collected at day 5 post-  
310 challenge showed no detectable levels of viral replication in the IN-vaccinated group.

311  
312 To measure vaccine protective efficacy in ferrets against completely heterosubtypic IAV  
313 challenge, two cohorts of vaccinated and mock-vaccinated ferrets were challenged with either  
314 A/H2N7 or A/H10N7 (Supplementary Table 2). Sequence identity of the challenge HA and NA  
315 subtypes as compared to the vaccine components ranged from 44.9-53.9%. Viral titers in nasal  
316 wash in IM- and IN-vaccinated A/H2N7-challenged ferrets were significantly reduced by day 5  
317 post-challenge (Fig. 3E), and lung titers collected at day 5 post-challenge showed no detectable  
318 levels of viral replication in both the IM- and IN-vaccinated groups. Similarly, challenge viral  
319 titers in ferret nasal wash in IM- and IN-vaccinated A/H10N7-challenged ferrets were significantly  
320 reduced by day 5 post-challenge (Fig. 3F). Lung titers collected at day 5 post-challenge showed

321 no detectable levels of viral replication in IN-vaccinated animals, while IM-vaccinated animals  
322 had viral titers that were not significantly reduced compared to mock-vaccinated animals.

323

324 **Host gene expression responses and qRT-PCR for viral RNA during mismatched and**  
325 **heterosubtypic challenge in ferrets.** To characterize the host gene expression response to viral  
326 challenge in PBS- and vaccinated mice, RNA expression microarray analysis and IAV M gene  
327 qRT-PCR was performed on lung tissue collected on day 5 post-challenge. ANOVA was  
328 performed to identify significantly differentially expressed genes ( $\geq 2$ -fold difference in median  
329 expression,  $p < 0.05$ ) between mock, IN and IM challenged animals. Due to the small number of  
330 animals, the analysis was performed with all 4 viruses in each group (mock-, IM- and IN-  
331 vaccinated). These sequences were enriched for pathways associated with the innate antiviral  
332 response, including IFN signaling, cytokine signaling, lymphocyte activation, and oxidative  
333 damage DNA repair responses (Fig, 4A) which were highly expressed in control animals but  
334 significantly lower in the IM- and IN-vaccinated animals (Fig. 4A), consistent with little viral  
335 replication in the lungs of these animals. No significant differences in lung gene expression  
336 responses were identified between IM- and IN-vaccinated, challenged ferrets.

337

338 **Lung pathology during mismatched and heterosubtypic viral challenge in ferrets.**  
339 Histopathological analysis was performed on ferret lung sections at day 5 post-viral challenge (Fig.  
340 4B and Supplementary Fig. S11-14). Lung sections of mock-vaccinated ferrets challenged with  
341 swine/Iowa/1931 (H1N1) virus showed marked pathological changes involving over 50% of the  
342 lung parenchyma, including multifocal, moderate-to-severe, necrotizing bronchitis and  
343 bronchiolitis (Fig. 4B and Supplementary Fig. S11), along with moderate-to-severe alveolitis with



344 a neutrophil-predominant, mixed inflammatory cell infiltrates, pulmonary edema and fibrinous  
345 exudates, a pathology remarkably similar to that seen with ferret infection with the 1918 pandemic  
346 H1N1 virus (23). Influenza viral antigen staining showed widespread positivity in respiratory  
347 epithelial cells and in alveolar epithelial cells. In contrast, lung sections from IM- and IN-  
348 vaccinated animals showed minimal histopathological changes, including mild, focal bronchiolitis,  
349 an absence of alveolitis and no viral antigen in alveolar epithelial cells.

350

351 Histopathological analysis was performed on ferret lung sections at day 5 post-viral challenge with  
352 the partially heterosubtypic A/Port Chalmers/1973 (A/H3N2) virus (Fig. 4B and Supplementary  
353 Fig S12). Lung sections of mock-vaccinated ferrets showed marked pathological changes  
354 involving over 50% of the lung parenchyma, including multifocal, moderate-to-severe, necrotizing  
355 bronchitis and bronchiolitis, along with moderate-to-severe alveolitis with a mixed inflammatory  
356 cell infiltrate, and focal pulmonary edema and fibrinous exudates. Influenza viral antigen staining  
357 showed widespread positivity in respiratory epithelial cells and in alveolar epithelial cells. In  
358 contrast, lung sections from IM- and IN-vaccinated animals showed no pneumonia, an absence of  
359 alveolitis, and no viral antigen in alveolar epithelial cells, while also showing multi-focal peri-  
360 bronchiolar lymphoid infiltrates.

361

362 Lung pathology from fully heterosubtypic viral challenges (with A/H2N7 and A/H10N7) were  
363 evaluated next. Lung sections of mock-vaccinated H2N7 challenged ferrets showed marked  
364 pathological changes (Fig. 4B and Supplementary Fig. S13) involving over 50% of the lung  
365 parenchyma, including multifocal, moderate-to-severe, necrotizing bronchitis and bronchiolitis,  
366 along with moderate-to-severe alveolitis with a mixed inflammatory cell infiltrate and numerous

367 intra-alveolar inflammatory cells. Influenza viral antigen staining showed widespread positivity  
368 in respiratory epithelial cells and in alveolar epithelial cells. Lung sections of mock-vaccinated  
369 H10N7 challenged ferrets showed marked pathological changes Fig. 4B and Supplementary Fig.  
370 S14), involving over 50% of the lung parenchyma, including multifocal, moderate-to-severe,  
371 necrotizing bronchitis and bronchiolitis, along with moderate-to-severe alveolitis with a  
372 neutrophil-predominant, mixed inflammatory cell infiltrate, numerous intra-alveolar inflammatory  
373 cells, and widespread pulmonary edema and fibrinous exudates. Influenza viral antigen staining  
374 showed widespread positivity in respiratory epithelial cells and in alveolar epithelial cells. In  
375 contrast, lung sections from IM- and IN-vaccinated animals challenged with H2N7 showed no  
376 pneumonia, bronchitis or bronchiolitis, but also showed prominent peri-bronchiolar lymphoid  
377 nodules. No alveolitis was noted and no influenza viral antigen was detected in alveolar epithelial  
378 cells in vaccinated ferrets (Supplementary Fig. S14). Similarly, lung sections from IM- and IN-  
379 vaccinated animals challenged with H10N7 showed no pneumonia, no bronchitis, bronchiolitis, or  
380 alveolitis. Peri-bronchiolar lymphoid nodules were observed. No influenza viral antigen was  
381 detected in alveolar epithelial cells, but as with H3N2 challenge above, some viral antigen was  
382 detected in bronchiolar respiratory epithelial cells in the absence of inflammation or  
383 histopathologic changes in IM-challenged animals, which may correspond to the detectable viral  
384 titers in 3 of 4 those animals (Fig. 3F). Similar to mouse studies, immunization with lower doses  
385 (1/4 antigen) provided protection against partially-heterosubtypic H3N2 and mismatched H1N1  
386 challenge in ferrets (Supplementary Fig S15), suggesting that a lower dose of the multivalent  
387 vaccine candidate could still provide a high level of protection.

388

389 **GMP manufacture, toxicology and immunogenicity studies.**

390 The systemic toxicity, local tolerance, and immunogenicity of the BPL influenza vaccine  
391 (administered IN or IM) was evaluated in New Zealand white rabbits. No mortality was observed  
392 following administration of the vaccine IN or IM. There were no clinical observations, injection  
393 or instillation site observations, changes in body weights, changes in food consumption, changes  
394 in body temperatures, systemic toxicity, local tolerance or ocular effects attributed to  
395 administration of the vaccine by either route. Rabbits that received the vaccine intranasally or  
396 intramuscular mounted serum antibody responses against the vaccine HA and NA antigens on day  
397 45 (Supplementary Fig. S16).

398

## 399 **Discussion**

400 A challenge to development of a “universal” influenza vaccine is the elicitation of effective broadly  
401 neutralizing antibodies and memory T cell responses. Currently, annual influenza virus vaccines  
402 are produced each year based on surveillance of circulating strains and predictions of which strains  
403 will be circulating the following season (24). While this approach can yield limited success, in  
404 many years strain-match predictions are imperfect and seasonal vaccines can be of limited  
405 effectiveness. Development of a “universal” influenza vaccine could be used as a super-seasonal  
406 vaccine that provides protection against new seasonal strains without the need for predictive  
407 antigenic matching, as well as provide protection against newly emerging pandemic and zoonotic  
408 influenza virus infections (7). Efforts to create a universal influenza vaccine have been ongoing  
409 for over four decades (12), while in the last five years this idea has gained renewed impetus from  
410 funders (7). Numerous strategies to achieve this goal are being currently pursued, including  
411 vaccines based on hemagglutinin head or stalk antigens, neuraminidase, the M2 protein  
412 exodomain, live attenuated influenza vaccines, and T cell-based vaccines targeting viral peptide

413 epitopes, as recently reviewed (25, 26). Several vaccine candidates have advanced into early  
414 clinical development (27-29), but whether these strategies will induce broad protection in humans  
415 has not yet been determined.

416

417 The approach taken in this study was to develop a broadly protective vaccine using beta-  
418 propiolactone (BPL) inactivated whole avian influenza viruses that contain full-length, properly  
419 folded HA and NA proteins, as well as other viral proteins (such as NP and M proteins) that have  
420 been shown to have conserved T cell epitopes (30). BPL-inactivated vaccines also have the  
421 advantage that they are simple and cheap to manufacture and have reduced cold-chain  
422 requirements. This study demonstrates that a broadly protective influenza vaccine, comprised of  
423 four BPL-inactivated whole low pathogenicity avian viruses, demonstrated near-universal  
424 protection from lethal viral infection against homologous, partially heterosubtypic, and completely  
425 heterosubtypic viral challenge in both mice and ferrets. For this vaccine, the four IAVs were  
426 chosen because they represent a broad consensus of the cladal HA and NA distribution of influenza  
427 A viruses. Avian IAV HA proteins also have low levels of glycosylation on the HA head as  
428 compared to human viruses, which allow for development of antibody responses against protein  
429 antigens that might be masked in seasonal IAVs. Moreover, because whole virions are used that  
430 likely provide T cell epitopes, vaccination should promote the development of broader memory T  
431 cell responses compared to purified vaccine antigens. The inactivated vaccine, delivered either  
432 IM or IN, is likely to be safe in humans as no toxicity was observed in mice or ferrets or in a rabbit  
433 toxicity study conducted as part of GMP manufacture.

434

435 In a prior study utilizing a vaccine consisting of a cocktail of four viral-like particles expressing  
436 the four HA proteins used here (20), broad protection against mismatched and completely  
437 heterosubtypic challenge was observed in mice. In this follow-up study, broad and potent  
438 protective efficacy was observed for a BPL-inactivated whole virus vaccine both in mouse and  
439 ferret model. Advantages of the current vaccine include ease of production, immunization with  
440 four HA antigens which induce systemic and respiratory antibodies against the HA heads and  
441 stalks, the addition of four divergent NA proteins which also induce systemic and respiratory  
442 antibodies, and internal viral proteins which likely serve as targets of T cell responses. Supporting  
443 this conclusion, the vaccine provided near 100% protective efficacy against mismatched or  
444 completely heterosubtypic challenge in mice and ferrets. In mice, vaccinated animals were  
445 protected against mismatched lethal challenge with pathogenic 1918 pandemic H1N1, H7N9,  
446 HPAI H5N8, and chimeric avian H7N1 virus challenges. Significantly, complete protection was  
447 afforded following challenge with the H6N1 virus, expressing a heterosubtypic HA (H6) not  
448 contained in the vaccine, and even more significantly, complete protection was observed following  
449 challenge with the fully heterosubtypic H10N7 virus, expressing both HA and NA subtypes not  
450 contained in the vaccine. Similarly, significant protection was observed in ferrets following  
451 completely heterosubtypic challenge with H2N7 or H10N7 viruses. These results are consistent  
452 with the desired characteristics of a “universal” influenza vaccine that could be of value in human  
453 vaccination programs.

454

455 Protective efficacy of vaccine-induced antibodies was evaluated in passive transfer of serum from  
456 mock-, IM-, or IN-vaccinated mice to naïve (unvaccinated) mice 1 day prior to lethal challenge  
457 with mismatched H7N1, partially heterosubtypic H6N1, or completely heterosubtypic H10N7

458 (Supplementary Fig. 9). Serum from IM-vaccinated mice afforded complete protection from  
459 H7N1 and partially heterosubtypic H6N1 virus lethal challenge, but not from completely  
460 heterosubtypic H10N7 challenge. Serum antibodies mediating survival following H6N1 challenge  
461 might include HA stalk antibodies, but protection was more likely provided by cross-reactive NA  
462 antibodies from the vaccine N1 antigen, since no serum protection was seen following completely  
463 heterosubtypic H10N7 challenge. These results demonstrate that a protective antibody response  
464 was generated against homologous IAV but suggest that other vaccine-induced immune  
465 mechanisms involving cellular immunity must be involved in protection against lethal challenge  
466 with heterosubtypic viruses.

467

468 In both IM- and IN-vaccinated mice and ferrets peri-bronchiolar and peri-vascular lymphoid  
469 aggregates were observed, and in mice it was possible to perform immunostaining to show that  
470 these aggregates contained both CD19<sup>+</sup> B and importantly, CD3<sup>+</sup> T lymphocytes. That IN-  
471 vaccinated mice and ferrets demonstrated potent protective efficacy even against completely  
472 heterosubtypic challenge despite mounting lower levels of serum antibody responses suggests that  
473 mucosal immunity plays an important role in anti-influenza virus responses, both through humoral  
474 and cellular immunity. As a further metric of vaccine effectiveness, vaccination was associated  
475 with a significant reduction in lung pathology and inflammatory gene expression responses in both  
476 mice and ferrets. The reduction in lung neutrophils during lethal challenge resulting from  
477 vaccination is likely critical to protection against lethal infection, as neutrophils and the ROS  
478 molecules they produce and excrete are major contributors to severe pulmonary pathology during  
479 fatal IAV infections (22, 31-33). Also concordant with reductions in viral replication and lung  
480 neutrophils, expression microarray analysis showed significant reductions in expression of genes

481 in type I IFN, ROS damage, and cell death pathways compared to mock-vaccinated and challenged  
482 mice and ferrets. In mice, increasing activation of these genes and associated pathways was  
483 observed with partially and completely heterosubtypic viral challenge in mice.

484

485 Further, the route of vaccination also affected lung host gene expression responses in mice. While  
486 both IM and IN vaccination were protective against lethal challenge in mice, expression analysis  
487 showed lower expression of inflammatory gene expression response pathways correlated with IM  
488 vaccination compared to IN vaccination. This vaccination route-dependent effect suggests that in  
489 mice mucosal or systemic vaccination affects molecular aspects of host immune responses, which  
490 arise from differences in effector functions or epithelial transport of IgA and IgG antibodies (34),  
491 or even a larger pool of adaptive immune cells in the periphery at vaccination. While both IM and  
492 IN vaccination were protective against lethal challenge in mice and ferrets, further studies are  
493 underway to better understand variables associated with the route of vaccination.

494

495 In summary, these preclinical studies in mice and ferrets demonstrate that a BPL-inactivated  
496 vaccine possesses many features of a successful universal influenza vaccine, with the potential to  
497 offer protection in human populations as a supra-seasonal and pre-pandemic IAV vaccine. In  
498 additional studies, humoral and cellular immune correlates of protection will be evaluated, as will  
499 vaccine efficacy in animals with a pre-existing exposure history to influenza A viruses to better  
500 mimic the complex immune repertoire exposure history to influenza viruses in humans, and  
501 whether vaccination results in reduction in transmission of influenza in ferrets.

502

503 **Acknowledgements**

504 This work was supported in part by the Intramural Research Programs of the National Institutes of  
505 Health and National Institute of Allergy and Infectious Diseases (NIAID) and in part by a grant  
506 from the Bill and Melinda Gates Foundation (OPP1178956). Animal care was performed by the  
507 Comparative Medicine Branch, NIH/NIAID. The rabbit toxicology study was performed under a  
508 contract from Battelle, with support of the Division of Microbiology and Infectious Diseases,  
509 NIAID.

510

#### 511 **Author contributions**

512 JP, LMS, KAW, MJM, JCK, and JKT conceived and designed the study. JKP, SF, LMS, ZMS,  
513 AF, LM, YX, MR, NB, LQ, LAR, SW, KS, MG, KAW, JKT generated the laboratory data. JKP,  
514 LMS, MR, NB, LQ, LAR, KS, MG, IB, DMM, KAW, MJM, JCK, and JKT interpreted the data.  
515 JKP, DMM, KAW, MJM, JCK, and JKT wrote the manuscript. All authors critically reviewed the  
516 paper and approved of the final version of the paper for submission.

517

#### 518 **Competing interests:**

519 A patent application describing the data presented in this paper has been filed by the National  
520 Institutes of Health.

521

522 **Data and materials availability:** The data and materials that support the findings of this study  
523 are available from the corresponding author upon reasonable request.

524

#### 525 **Supplementary Materials**

526 Materials and Methods

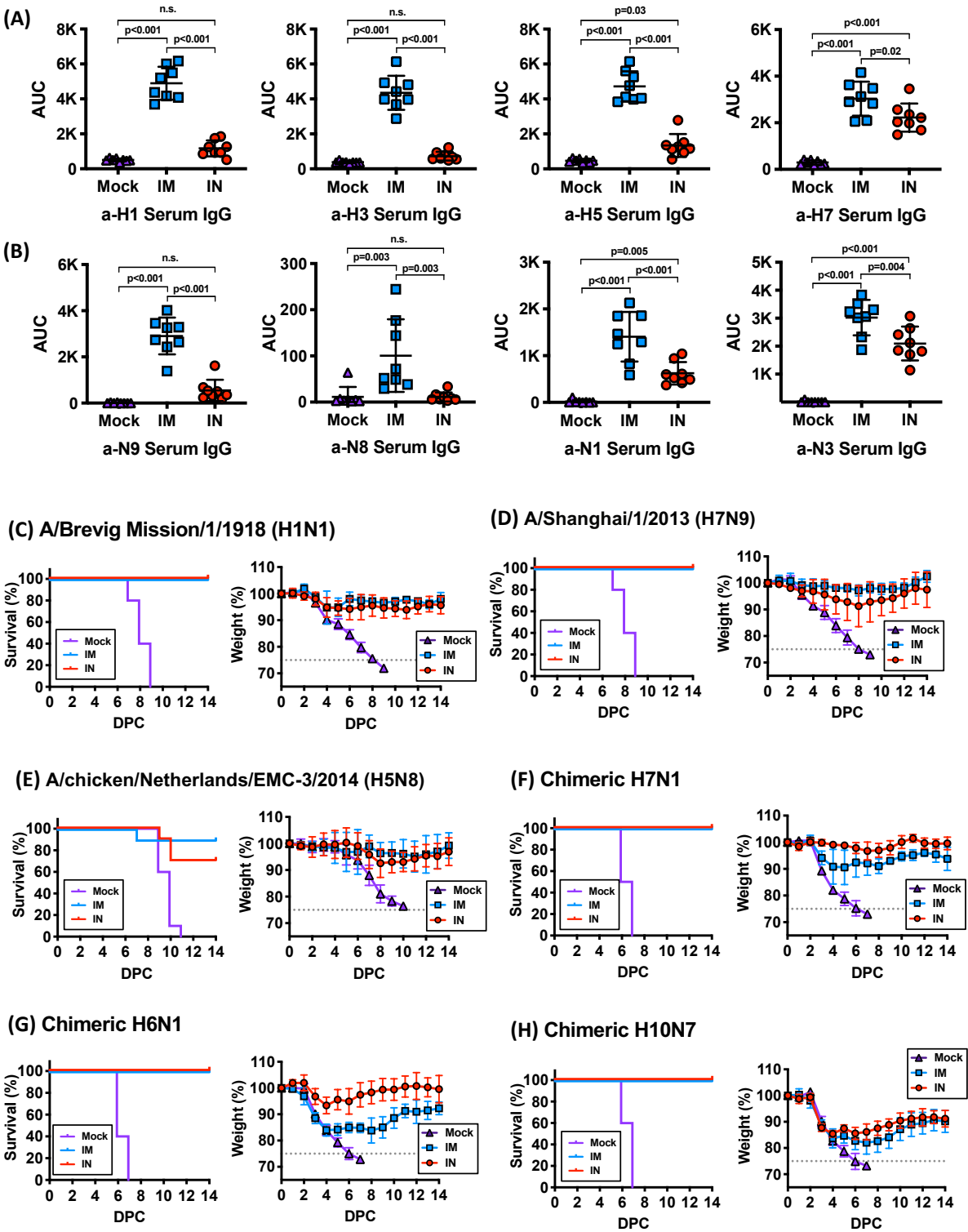


527 Supplementary Figures. S1 to S16

528 Supplementary Tables S1 to S2

529

530

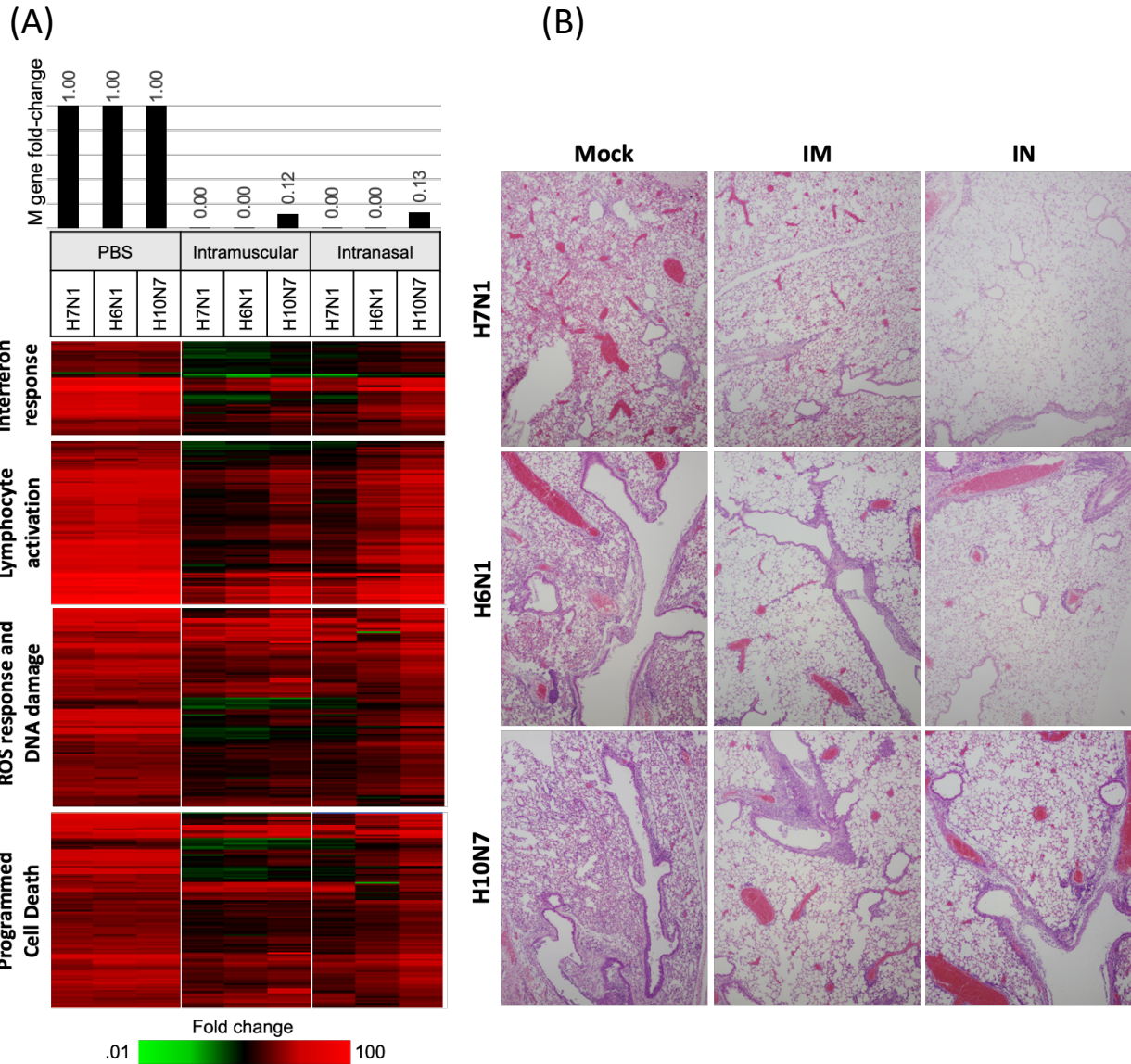


531

532 **Figure 1. Immunogenicity and protective efficacy of the BPL-inactivated vaccine in mice.**

533 Serum IgG levels against (A) four vaccine hemagglutinin (HA) antigens and (B) four vaccine

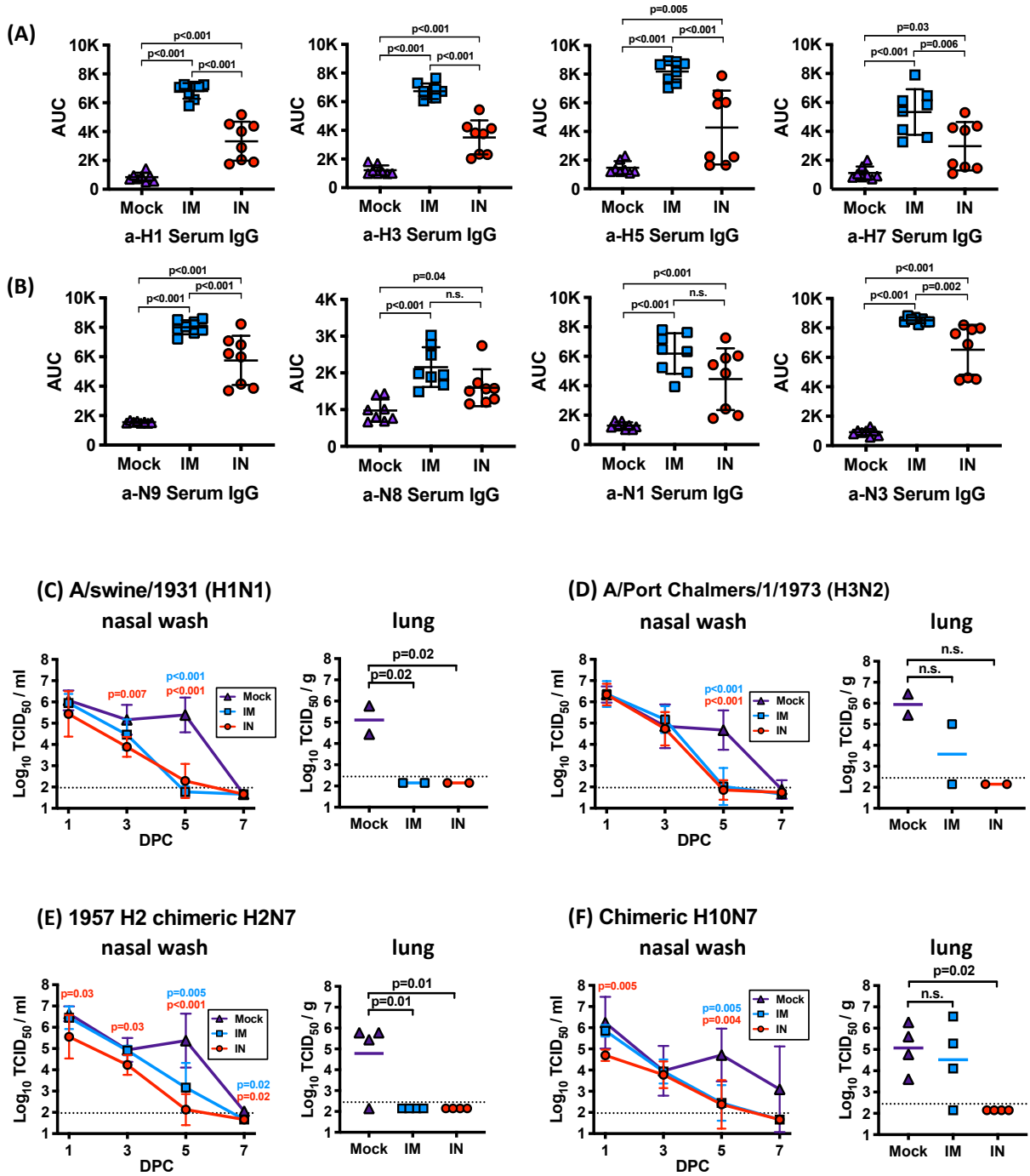
534 neuraminidase (NA) antigens were measured 3 weeks after the boost immunization in mock-, IM-  
535 , or IN-vaccinated mice using ELISA. Ordinary ANOVA test and post hoc Tukey's multiple  
536 comparison test were used to compared antibody levels between groups. n.s; not significant (**C-**  
537 **F**). Percent survival and percent weight loss in mock-, IM-, or IN-vaccinated mice after lethal  
538 challenge (10xLD<sub>50</sub>) with six different influenza A virus challenge strains: (**C**) 1918 pandemic  
539 H1N1, (**D**) H7N9, (**E**) highly pathogenic avian H5N8, (**F**) chimeric avian H7N1, (**G**) chimeric  
540 avian H6N1, and (**H**) chimeric H10N7 virus. Error bars represent standard deviation. n.s; not  
541 significant  
542



543

544 **Figure 2. Quantitative RT-PCR for influenza viral RNA, lung inflammatory responses, and**  
 545 **histopathology of vaccinated mice. (A)** Top panel, bar graph showing relative expression of IAV  
 546 M gene mRNA in vaccinated mouse lung compared to mock-vaccinated animals as measured by  
 547 qRT-PCR. Lower panels, differences in lung gene expression responses in lungs of mock, IM,  
 548 and IN vaccinated mice identified by ANOVA ( $\geq 2$ -fold difference in median expression level,  
 549  $p < 0.01$ ) on day 6 post-challenge with heat maps show the relative expression of type I interferon  
 550 response, lymphocyte activation, ROS response and DNA damage, and programmed cell death.

551 Genes with increased expression are show in red, genes with no change as black, and genes  
552 showing decreased expression in green. **(B)** Lung histopathology of mock-, IM-, and IN-  
553 vaccinated mice lethally challenged with chimeric avian H6N1, H7N1, or H7N10 viruses  
554 (10xLD<sub>50</sub> dose), and analyzed at day 5 post-infection. In each case, mock-vaccinated animals  
555 showed a widespread, severe viral pneumonia with necrotizing bronchitis and bronchiolitis,  
556 alveolitis. In contrast, IM- or IN-vaccinated animals showed an absence of pneumonia, with no  
557 bronchitis, bronchiolitis, or alveolitis. Aggregates of lymphoid tissue were observed in peri-  
558 bronchiolar and peri-bronchiolar spaces in vaccinated animals. Original magnifications 20x. See  
559 Supplementary Figs 5-7 for additional pathological analyses.  
560



561

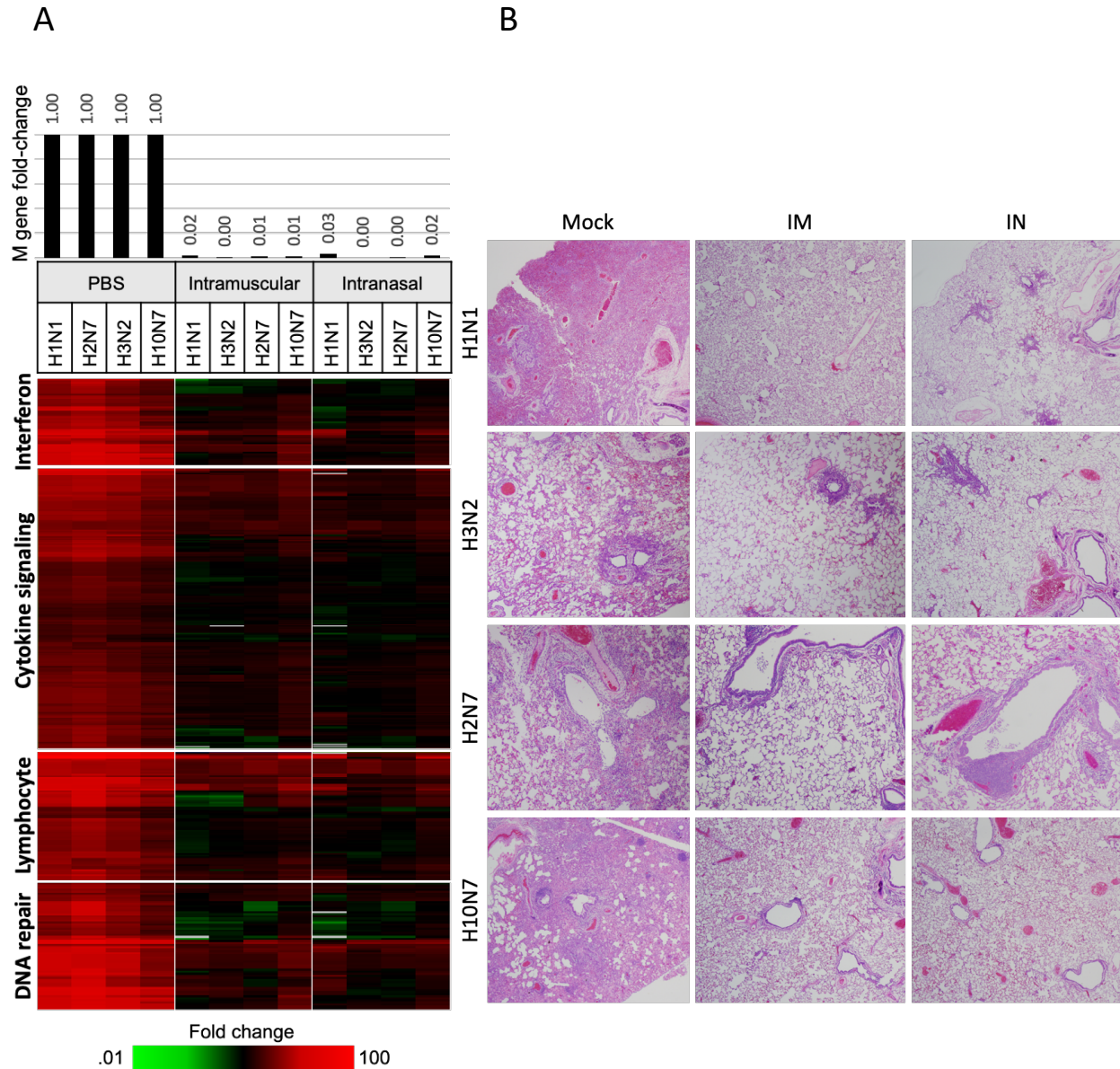
562 **Figure 3. Immunogenicity and reduction in viral titers of BPL-inactivated vaccinated**

563 **ferrets.** Serum IgG levels against (A) four vaccine hemagglutinin (HA) antigens and (B) four

564 vaccine neuraminidase (NA) antigens were measured 3 weeks after the boost immunization in

565 mock-, IM-, or IN-vaccinated mice using ELISA. Ordinary ANOVA test and post hoc Tukey's

566 multiple comparison test were used to compared antibody levels between groups. Error bars  
567 represent standard deviation. **(C-F)**. Reductions in nasal wash and lung viral titers in IM- or IN-  
568 vaccinated ferrets as compared to mock-vaccinated ferrets. Nasal wash titers were measured at  
569 days 1, 3, 5, and 7 following challenge, and lung titers were determined on day 5 following  
570 challenge. **(C)**. Reductions in titers following A/swine/1931 (H1N1) challenge. **(D)**. Reductions  
571 in titers following A/Port Chalmers/1/1973 (H3N2) challenge. **(E)**. Reductions in titers following  
572 chimeric 1957 pandemic H2N7 challenge. **(F)**. Reductions in titers following chimeric avian  
573 H10N7 challenge. Ordinary ANOVA test and post hoc Dunnett's multiple comparison test were  
574 used to compare viral titers in IM- or IN-vaccinated ferrets to mock-vaccinated ferrets. Error bars  
575 represent geometric standard deviation. n.s; not significant  
576



577

578 **Figure 4. Quantitative RT-PCR for influenza viral RNA, lung inflammatory responses, and**

579 **histopathology of vaccinated ferrets. (A)** Top panel, bar graph showing relative expression of

580 IAV M gene mRNA in vaccinated ferret lung compared to mock-vaccinated animals as measured

581 by qRT-PCR. Lower panels, differences in lung gene expression responses in lungs of mock, IM,

582 and IN vaccinated ferrets identified by ANOVA ( $\geq 2$ -fold difference in median expression level,

583  $p < 0.01$ ) on day 5 post-challenge with heat maps show the relative expression of type I interferon



584 responses, cytokine signaling, lymphocyte activation, and DNA repair. **(B)** Lung histopathology  
585 of mock-, IM-, and IN-vaccinated mice lethally challenged with A/swine/1931 (H1N1), A/Port  
586 Chalmers/1/1973 (H3N2), or completely heterosubtypic challenge with chimeric H2N7 or H10N7  
587 challenge viruses. In each case, mock-vaccinated animals showed a widespread, severe viral  
588 pneumonia with necrotizing bronchitis and bronchiolitis, alveolitis. In contrast, IM- or IN-  
589 vaccinated animals showed an absence of pneumonia, with no bronchitis, bronchiolitis, or  
590 alveolitis. Aggregates of lymphoid tissue were observed in peri-bronchiolar and peri-bronchiolar  
591 spaces in vaccinated animals. Original magnifications 20x. See Supplementary Figs S11-14 for  
592 additional pathological analyses.  
593

594 **References**

595

- 596 1. A. D. Iuliano *et al.*, Estimates of global seasonal influenza-associated respiratory mortality:  
597 a modelling study. *Lancet* **391**, 1285-1300 (2018).
- 598 2. V. G. Dugan *et al.*, The evolutionary genetics and emergence of avian influenza viruses in  
599 wild birds. *PLoS Pathog* **4**, e1000076 (2008).
- 600 3. J. K. Taubenberger, D. M. Morens, Influenza: the once and future pandemic. *Public Health*  
601 *Rep* **125 Suppl 3**, 16-26 (2010).
- 602 4. N. P. Johnson, J. Mueller, Updating the accounts: global mortality of the 1918-1920  
603 "Spanish" influenza pandemic. *Bull Hist Med* **76**, 105-115 (2002).
- 604 5. C. Hannoun, The evolving history of influenza viruses and influenza vaccines. *Expert Rev*  
605 *Vaccines* **12**, 1085-1094 (2013).
- 606 6. J. K. Park, J. K. Taubenberger, Universal Influenza Vaccines: To Dream the Possible  
607 Dream? *ACS Infect Dis* **2**, 5-7 (2016).
- 608 7. E. J. Erbeiding *et al.*, A Universal Influenza Vaccine: The Strategic Plan for the National  
609 Institute of Allergy and Infectious Diseases. *J Infect Dis* **218**, 347-354 (2018).
- 610 8. N. M. Bouvier, P. Palese, The biology of influenza viruses. *Vaccine* **26 Suppl 4**, D49-53  
611 (2008).
- 612 9. J. K. Taubenberger, J. C. Kash, Influenza virus evolution, host adaptation, and pandemic  
613 formation. *Cell Host Microbe* **7**, 440-451 (2010).
- 614 10. B. Olsen *et al.*, Global patterns of influenza A virus in wild birds. *Science* **312**, 384-388  
615 (2006).
- 616 11. D. M. Morens, J. K. Taubenberger, A. S. Fauci, Pandemic influenza viruses--hoping for  
617 the road not taken. *N Engl J Med* **368**, 2345-2348 (2013).
- 618 12. G. M. Air, W. G. Laver, R. G. Webster, Towards a universal influenza vaccine. *Prog Clin*  
619 *Biol Res* **47**, 193-215 (1980).
- 620 13. V. A. Slepishkin *et al.*, Protection of mice against influenza A virus challenge by  
621 vaccination with baculovirus-expressed M2 protein. *Vaccine* **13**, 1399-1402 (1995).
- 622 14. D. Mezhenkaya, I. Isakova-Sivak, L. Rudenko, M2e-based universal influenza vaccines:  
623 a historical overview and new approaches to development. *J Biomed Sci* **26**, 76 (2019).
- 624 15. J. L. Schulman, M. Khakpour, E. D. Kilbourne, Protective effects of specific immunity to  
625 viral neuraminidase on influenza virus infection of mice. *J Virol* **2**, 778-786 (1968).
- 626 16. L. T. Giurgea, D. M. Morens, J. K. Taubenberger, M. J. Memoli, Influenza Neuraminidase:  
627 A Neglected Protein and Its Potential for a Better Influenza Vaccine. *Vaccines (Basel)* **8**,  
628 (2020).
- 629 17. M. Koutsakos *et al.*, Human CD8(+) T cell cross-reactivity across influenza A, B and C  
630 viruses. *Nat Immunol* **20**, 613-625 (2019).
- 631 18. H. M. Yassine *et al.*, Hemagglutinin-stem nanoparticles generate heterosubtypic influenza  
632 protection. *Nat Med* **21**, 1065-1070 (2015).
- 633 19. F. Krammer, N. Pica, R. Hai, I. Margine, P. Palese, Chimeric hemagglutinin influenza virus  
634 vaccine constructs elicit broadly protective stalk-specific antibodies. *J Virol* **87**, 6542-6550  
635 (2013).
- 636 20. L. M. Schwartzman *et al.*, An Intranasal Virus-Like Particle Vaccine Broadly Protects  
637 Mice from Multiple Subtypes of Influenza A Virus. *mBio* **6**, e01044 (2015).
- 638 21. M. Kanekiyo *et al.*, Mosaic nanoparticle display of diverse influenza virus hemagglutinins  
639 elicits broad B cell responses. *Nat Immunol* **20**, 362-372 (2019).

- 640 22. L. Qi *et al.*, Contemporary avian influenza A virus subtype H1, H6, H7, H10, and H15  
641 hemagglutinin genes encode a mammalian virulence factor similar to the 1918 pandemic  
642 virus H1 hemagglutinin. *mBio* **5**, e02116 (2014).
- 643 23. M. J. Memoli *et al.*, An early 'classical' swine H1N1 influenza virus shows similar  
644 pathogenicity to the 1918 pandemic virus in ferrets and mice. *Virology* **393**, 338-345  
645 (2009).
- 646 24. C. A. Russell *et al.*, Influenza vaccine strain selection and recent studies on the global  
647 migration of seasonal influenza viruses. *Vaccine* **26 Suppl 4**, D31-34 (2008).
- 648 25. R. Nachbagauer, F. Krammer, Universal influenza virus vaccines and therapeutic  
649 antibodies. *Clin Microbiol Infect* **23**, 222-228 (2017).
- 650 26. C. I. Paules, A. S. Fauci, Influenza Vaccines: Good, but We Can Do Better. *J Infect Dis*  
651 **219**, S1-S4 (2019).
- 652 27. D. I. Bernstein *et al.*, Immunogenicity of chimeric haemagglutinin-based, universal  
653 influenza virus vaccine candidates: interim results of a randomised, placebo-controlled,  
654 phase 1 clinical trial. *Lancet Infect Dis* **20**, 80-91 (2020).
- 655 28. E. van Doorn *et al.*, Evaluating the immunogenicity and safety of a BiondVax-developed  
656 universal influenza vaccine (Multimeric-001) either as a standalone vaccine or as a primer  
657 to H5N1 influenza vaccine: Phase IIb study protocol. *Medicine (Baltimore)* **96**, e6339  
658 (2017).
- 659 29. O. Pleguezuelos *et al.*, Efficacy of FLU-v, a broad-spectrum influenza vaccine, in a  
660 randomized phase IIb human influenza challenge study. *NPJ Vaccines* **5**, 22 (2020).
- 661 30. A. Schmidt, D. Lapuente, T Cell Immunity against Influenza: The Long Way from Animal  
662 Models Towards a Real-Life Universal Flu Vaccine. *Viruses* **13**, (2021).
- 663 31. B. M. Tang *et al.*, Neutrophils-related host factors associated with severe disease and  
664 fatality in patients with influenza infection. *Nat Commun* **10**, 3422 (2019).
- 665 32. T. M. Tumpey *et al.*, Pathogenicity of influenza viruses with genes from the 1918 pandemic  
666 virus: functional roles of alveolar macrophages and neutrophils in limiting virus replication  
667 and mortality in mice. *J Virol* **79**, 14933-14944 (2005).
- 668 33. J. C. Kash *et al.*, Treatment with the reactive oxygen species scavenger EUK-207 reduces  
669 lung damage and increases survival during 1918 influenza virus infection in mice. *Free  
670 Radic Biol Med* **67**, 235-247 (2014).
- 671 34. *Immunobiology: The Immune System in Health and Disease. 5th edition. The distribution  
672 and functions of immunoglobulin isotypes. Available from:  
673 <https://www.ncbi.nlm.nih.gov/books/NBK27162/>. (Garland Science, New York, 2001).*  
674

# Supplementary Materials for

## **An inactivated multivalent influenza A virus vaccine is broadly protective in mice and ferrets**

Jaekeun Park, Sharon Fong, Louis M. Schwartzman, Zhong-Mei Sheng, Ashley Freeman, Lex Matthews, Yongli Xiao, Mitchell D. Ramuta, Natalia A. Batchenkova, Li Qi, Luz Angela Rosas, Stephanie Williams, Kelsey Scherler, Monica Gouzoulis, Ian Bellayr, David M. Morens, Kathie-Anne Walters, Matthew J. Memoli, John C. Kash, and Jeffery K. Taubenberger\*

\*Correspondence to: [taubenbergerj@niaid.nih.gov](mailto:taubenbergerj@niaid.nih.gov)

### **This PDF file includes:**

Materials and Methods

Supplementary Figures. S1 to S16

Supplementary Tables S1 to S2

References

## 19 **Materials and Methods**

### 20 **Quadrivalent vaccine design and construction**

21 Low pathogenicity avian viruses A/mallard/Ohio/265/1987 (H1N9),  
22 A/pintail/Ohio/339/1987 (H3N8), A/mallard/Maryland/802/2007 (H5N1), and  
23 A/Environment/Maryland/261/2006 (H7N3) were grown in MDCK cells followed by inactivation  
24 using  $\beta$ -propiolactone (BPL; catalog no. P5648; MilliporeSigma, USA). Viral culture supernatant  
25 was buffered with HEPES (catalog no. 15630; ThermoFisher, USA) at a final concentration of  
26 0.1M and BPL was added (0.1% final). After overnight incubation at 4°C for the viral inactivation,  
27 BPL was hydrolyzed at 37°C for 90 min. Inactivated viruses were concentrated by  
28 ultracentrifugation at 50,000xg for 2h and purified using a 20-60% (w/v) discontinuous sucrose  
29 density gradient purification (100,000xg, 2h). A band at the 20-60% sucrose interface containing  
30 purified viruses was collected and the sucrose was removed by pelleting viruses (50,000xg, 2h)  
31 followed by virus resuspension in PBS. The total protein amount of the purified viruses was  
32 quantified using a bicinchoninic acid (BCA) protein assay kit (catalog no. 23225; ThermoFisher).  
33 For intranasal immunization in mice, 1 dose of vaccine was formulated to contain 1.5ug of each  
34 antigen (6ug total) in 50ul PBS. For intramuscular immunization in mice, 1 dose of vaccine was  
35 formulated to contain 1.5ug of each antigen (6ug total) in 25ul PBS and supplemented with 25ul  
36 of adjuvant AddaVax (catalog no. vac-adx-10; InvivoGen, USA). For the ferret study, 100ug of  
37 each antigen (400ug total) in 1ml PBS was used for 1 dose of intranasal immunization. For  
38 intramuscular immunization in ferrets, 100ug of each antigen (400ug total) in 250ul PBS was  
39 supplemented with 250ul of AddaVax (catalog no. vac-adx-10; InvivoGen). Low dose vaccines  
40 are prepared as described above, but with 1/4 antigen (i.e. 1.5ug total for mice, 100ug total for  
41 ferrets).

42

### 43 **Challenge viruses**

44 Fully reconstructed 1918 pandemic H1N1 virus was generated using a 12-plasmid reverse  
45 genetics system as previously described (1, 2) and passaged in MDCK cells. Avian influenza  
46 viruses (H6N1, H7N1, and H10N7) and recombinant H2N7 virus containing the 1957 H2  
47 pandemic HA were generated as previously described (1, 3). A/Swine/Iowa/1931 (H1N1), A/Port  
48 Chalmers/1/1973 (H3N2), A/chicken/Netherlands/EMC-3/2014 (H5N8), and A/Shanghai/1/2013  
49 (H7N9) viruses were passaged in embryonated specific-pathogen-free (SPF) chicken eggs (catalog  
50 no. 10100329; Charles River, USA). Supplementary Table 2 summarizes the challenge viruses  
51 used in this study and the hemagglutinin (HA) and neuraminidase (NA) identity to vaccine virus  
52 components. All viruses and infectious samples were handled under enhanced biosafety level 3  
53 (BSL-3) laboratory conditions except for A/Swine/Iowa/1931 (H1N1) A/Port Chalmers/1/1973  
54 (H3N2) which were handled in BSL-2 laboratory conditions. Experiments with the fully  
55 reconstructed 1918 pandemic virus and the highly pathogenic avian influenza (HPAI) H5N8 virus  
56 were conducted in accordance with the select agent guidelines of the National Institutes of Health  
57 (NIH), the Centers for Disease Control and Prevention and the United States Department of  
58 Agriculture, under the supervision of the NIH Select Agent and Biosurety Programs and the NIH  
59 Department of Health and Safety.

60

### 61 **Mouse studies**

62 Seven-to-eight-week-old female BALB/C mice (Jackson Laboratories, USA) were lightly  
63 anesthetized with isoflurane supplemented with O<sub>2</sub> (1.5 L/min) before immunization or virus  
64 challenge. Mice were intranasally or intramuscularly immunized twice 4 weeks apart with the

65 quadrivalent vaccines prepared as described above. Mock-vaccinated control mice received PBS  
66 or adjuvant without antigen. Serum samples were collected 3 weeks after the boost immunization  
67 to measure antibody responses elicited by the immunization. Lethal challenge infections (10x  
68 LD50 dose in 50ul inoculum per animal) were performed 4 weeks after the boost immunization.  
69 Post-challenge body weight and survival were monitored for 14 days from 5 mice/experimental  
70 condition. Ten mice, instead of 5, were used for the HPAI H5N8 challenge study. Mice were  
71 humanely euthanized if more than 25% of initial body weight was lost. For measuring viral loads  
72 and transcriptomics from H7N1, H6N1, and H10N7 challenge groups, lungs were harvested at day  
73 6 (n=4) post-infection and immediately frozen in dry ice and stored at -80°C until processed. For  
74 histopathology, lungs were harvested at day 5 post-infection (n=2) followed by inflation and  
75 fixation using 10% neutral buffered formalin (NBF).

76

### 77 **Ferret studies**

78 Five-to-seven-month-old female ferrets (Triple F Farms, USA) were lightly anesthetized  
79 with isoflurane supplemented with O<sub>2</sub> (1.5 L/min) before immunization or virus challenge. Ferrets  
80 were intranasally or intramuscularly immunized twice 4 weeks apart with the quadrivalent  
81 vaccines prepared as described above. Mock-vaccinated control ferrets received PBS or the  
82 adjuvant. Serum samples were collected 3 weeks after the boost immunization to measure  
83 antibody responses elicited by the immunization. Challenge infections (1ml inoculum per animal)  
84 were performed 4 weeks after the boost immunization. For A/swine/1931 (H1N1) and A/Port  
85 Chalmers/1973 (H3N2) challenge, 1x10<sup>7</sup> plaque-forming unit (PFU) of each virus was used. For  
86 chimeric H2N7 and H10N7 challenge, 2x10<sup>5</sup> PFU of each virus was used. To measure viral  
87 shedding in the upper respiratory tract following infection, nasal wash samples were collected at

88 days 1, 3, 5, and 7 post-infection using 1ml of PBS. To measure viral shedding, transcriptomics,  
89 and histopathology in the lower respiratory tract, ferrets were euthanized at day 5 post-challenge  
90 and lungs were harvested. Left cranial lobes of the harvested lungs were immediately frozen in dry  
91 ice and stored at  $-80^{\circ}\text{C}$  until processed for measuring viral loads and transcriptomics. For  
92 histopathology, remaining lungs were inflated and fixed using 10% NBF. All experimental animal  
93 work was performed in accordance with United States Public Health Service (PHS) Policy on  
94 Humane Care and Use of Laboratory Animals in an ABSL2 laboratory or an enhanced animal  
95 BSL3 (ABSL-3+) laboratory (for the viral challenge) as necessary at the National Institute of  
96 Allergy and Infectious Diseases (NIAID) of the NIH following approval of animal safety protocols  
97 by the NIAID Animal Care and Use Committee.

98

### 99 **RNA isolation and expression microarray analysis**

100 Frozen lungs, collected as described above, were lightly defrosted, homogenized in Trizol  
101 (catalog no. 15596018; ThermoFisher), and total RNA was isolated following manufacturer's  
102 protocol. Isolated total RNA was purified using RNeasy Mini Kit (catalog no. 74106; Qiagen,  
103 Germany). Gene expression profiling experiments were performed using Agilent Mouse Whole  
104 Genome 44K microarrays (catalog no. G4122F; Agilent, USA). Ferret expression microarray  
105 analysis was performed using custom microarrays from Agilent Technologies (4). Fluorescent  
106 probes were prepared using Agilent QuickAmp Labeling Kit (catalog no. 5190-2305; Agilent)  
107 according to the manufacturer's instructions. Each RNA sample was labeled and hybridized to  
108 individual arrays. Spot quantitation was performed using Agilent's Feature Extractor software and  
109 all data were uploaded into Genedata Analyst 9.0 (Genedata, Switzerland). Data normalization  
110 was performed in Genedata Analyst 9.0 (Genedata) using central tendency followed by relative



111 normalization using pooled RNA from mock infected mouse lung (n=4) or ferret lung (n=3) as a  
112 reference. Transcripts showing differential expression (2-fold,  $p < 0.01$ ) between infected and  
113 control animals were identified by standard t test. The Benjamini-Hochberg procedure was used  
114 to correct for false positive rate in multiple comparisons. Panther and Ingenuity Pathway Analysis  
115 (IPA) was used for gene ontology and pathway classification [A-B].

116

### 117 **Viral load determination in mouse and ferret lungs**

118 Influenza viral titers in mouse and ferret lungs were quantified using qPCR from the RNA  
119 samples prepared as described above. Reverse transcription of total RNA was performed using  
120 the Superscript III first-strand cDNA synthesis kit (catalog no. 18080051; ThermoFisher) primed  
121 with an equal mix of oligo(dT) and the Uni12 influenza A specific primer: 5' AGCRAAAGCAGG  
122 3'. The IAV matrix gene amplicon was quantified using the following primers and probe  
123 sequences: forward primer, 5'-ARATGAGTCTTCTRACCGAGGTCG-3'; reverse primer, 5'-  
124 TGCAAAGACATCYTCAAGYYTCTG-3'; probe, 5'-[6-FAM]  
125 TCAGGCCCCCTCAAAGCCGA [BHQ1]-3' (5, 6). Real-time PCR was performed on a Bio-Rad  
126 CFX384 Touch Real-Time PCR Detection System with TaqMan 2X PCR Universal Master Mix  
127 using a 10uL total reaction volume in duplicate. Ct values were normalized to the calibrator gene  
128 mouse GAPDH (catalog no. 4352932E; ThermoFisher).

129

### 130 **Viral load determination in ferret nasal wash**

131 Viral loads of ferret nasal wash samples were measured using 50% Tissue Culture  
132 Infectious Dose (TCID<sub>50</sub>) assay in MDCK cells. Reed and Muench method (7) was used for the  
133 TCID<sub>50</sub> calculation.

134

135 **Immunogenicity**

136 Serum samples collected approximately three weeks post-boost immunization were used  
137 to investigate the immunogenicity of the quadrivalent vaccine. Hemagglutination inhibition (HAI)  
138 assay was performed as previously described (8). Enzyme-linked immunosorbent assay (ELISA)  
139 was also used to measure antibodies recognizing homologous HAs (H1, H3, H5, H7) and NAs  
140 (N1, N3, N8, N9) using recombinant HA and NA proteins. Antibodies recognizing group1 and  
141 group2 HA stalk were also measured. Recombinant proteins for the ELISA were designed based  
142 on previously published HA (9), NA (10), group 1 HA stalk (11), and group2 HA stalk (12)  
143 constructs with a Strep-Tag II affinity tag. Particularly, for the group 2 HA stalk, a chimeric HA  
144 consisting of a globular head of H4 HA and a stalk of H3 HA (cH4/3) was used. The recombinant  
145 proteins were expressed in insect cells, purified using Strep-Tactin Sepharose (catalog no. 2-1201;  
146 IBA GmbH, Germany), and quantified using BCA protein assay kit (catalog no. 23225;  
147 ThermoFisher) as previously described (11). Purified proteins were diluted in PBS (1µg/ml) and  
148 added to 96-well ELISA plates (50µl/well) (catalog no. 456537; ThermoFisher). The plates were  
149 incubated overnight at 4°C followed by the addition of blocking buffer (1% BSA in PBS,  
150 100µl/well). After 30 min at room temperature, the plates were washed three times with wash  
151 buffer (0.05% Tween 20 in PBS). Serum samples were serially diluted in antibody diluent (1%  
152 BSA and 0.05% Tween 20 in PBS) and added to the washed plates (50µl/well). After incubation  
153 (RT, 2 h), the plates were washed three times and 1:10,000 diluted HRP-conjugated anti-mouse  
154 IgG antibody (catalog no. A28177; ThermoFisher) or anti-ferret IgG antibody (catalog no.  
155 ab112770; Abcam, USA) were added (100µl/well). After incubation (RT, 1h), the plates were  
156 washed six times followed by 30 min RT incubation with HRP substrate solution (100µl/well)

157 prepared by adding a 10mg o-phenylenediamine dihydrochloride (OPD) tablet (catalog no. P8287;  
158 MilliporeSigma) to 20ml of phosphate-citrate buffer preparation (catalog no. P4922;  
159 MilliporeSigma). The reaction was stopped by adding 1 M sulfuric acid (100  $\mu$ l/well), and the  
160 optical density was measured at 492 nm (OD492). Area under the curve (AUC) values were  
161 calculated using Prism8 software v.8.4.3 (GraphPad Software, USA). The baseline for AUC  
162 calculation was set as 0.1 to exclude non-specific signals from the AUC calculation. The OD492  
163 of 0.1 is approximately 2 times the OD492 value from the control wells that were treated equally,  
164 but without the addition of diluted serum. Reciprocal dilutions (dilution factors) of the serum were  
165 used as x-values for the AUC calculation. Additionally, the level of secretory IgA in mice was  
166 also measured from bronchoalveolar lavage (BAL) fluid collected approximately three weeks-post  
167 boost immunization. The BAL fluids were serially diluted, and the level of IgA was measured as  
168 described above. HRP-conjugated anti-mouse IgA antibody (catalog no. ab97235; Abcam) was  
169 used.

170

### 171 **Histopathology and immunohistochemistry**

172 NBF-fixed mouse and ferret lungs were processed for histopathology and  
173 immunohistochemistry as previously described (13). Hematoxylin and eosin (H&E)-stained slides  
174 were examined from two mice or four ferrets per virus group at 5 days post-infection.  
175 Immunohistochemistry was done on the same sets of fixed tissues as the histopathology. For the  
176 mouse lung tissues, Influenza A virus and immune cell (neutrophil, B and T cells) distribution  
177 were measured by immunohistochemistry. A goat polyclonal primary anti-influenza A virus  
178 (catalog no. ab20841; Abcam, USA) was used to stain influenza NP proteins. Anti-CD19 antibody  
179 (catalog no. 90176S; Cell Signaling Technology, USA), anti-CD3 antibody (catalog no. ab16669;

180 Abcam), and anti-Ly6G antibody (catalog no. ab210204; Abcam) were used to stain B cells, T  
181 cells, and neutrophils, respectively. For the ferret lung tissues, only Influenza A virus distribution  
182 was measured by immunohistochemistry. All slides were scanned on an Aperio ScanScope XT  
183 system (Aperio, USA), enabling whole-slide analysis.

184

### 185 **Statistics**

186 Prism8 software v.8.4.3 (GraphPad Software) was used for statistical evaluations of  
187 antibody levels and viral titers by ordinary ANOVA test. Tukey's multiple comparison test was  
188 used as post hoc test to compared antibody levels between groups. Viral titers of the IM and IN  
189 groups were log-transformed and compared to Mock group using Dunnett's multiple comparison  
190 test as post hoc test. Hierarchical clustering and additional analyses were performed using TIBCO  
191 Spotfire® Analyst 7.6.0 (TIBCO Software, Palo Alto, CA).

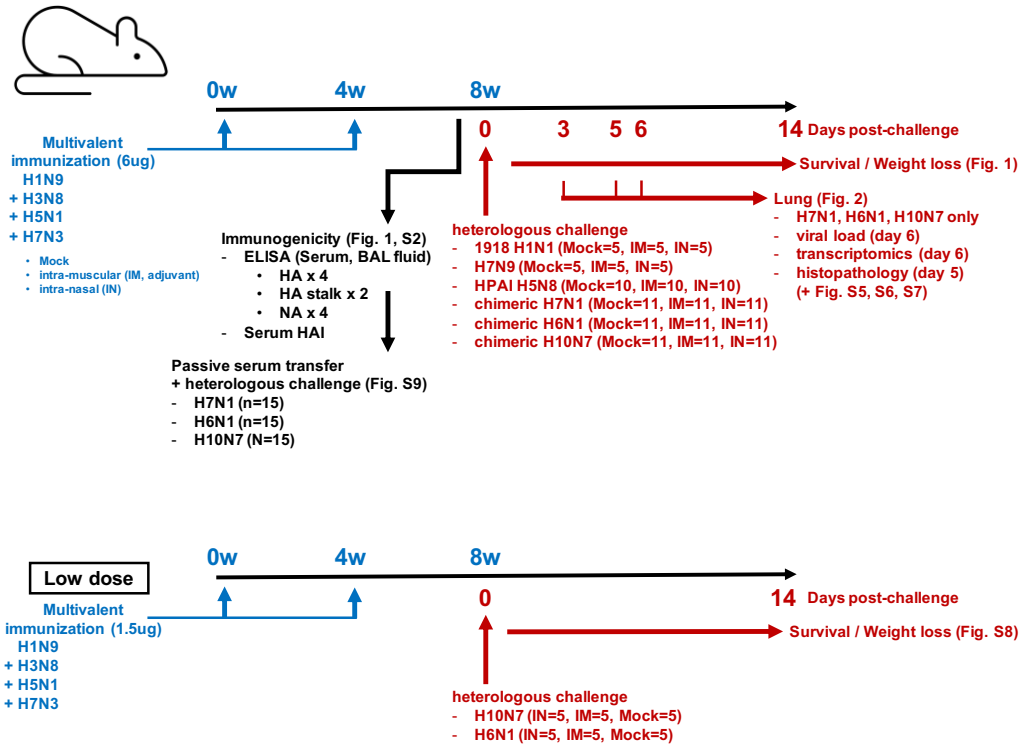
192

### 193 **GMP manufacture and toxicology studies**

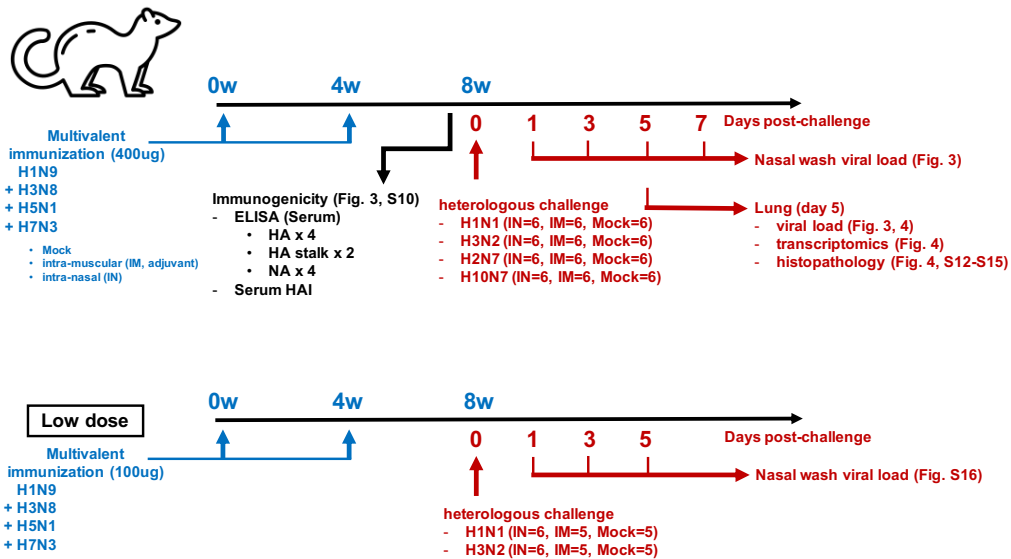
194 The four vaccine virus (Supplementary Table 1) seed stocks were used for Good  
195 Manufacturing Practice (GMP) manufacturing of the vaccine components in certified Vero cells.  
196 A rabbit toxicology and immunogenicity study were performed under contract by Batelle. Thirty  
197 4-to-7 month old New Zealand White Rabbits (2 to 4 kg) were employed for the study. A group  
198 of 10 animals received saline administered by IN (240 µL; 120 µL per naris) and IM (n = 10; 5  
199 male & 5 female), another group of 10 received the GMP-manufactured vaccine IN (20ug of each  
200 antigen; 80ug total), and the final group of 10 received the GMP-manufactured vaccine IM (20ug  
201 of each antigen; 80ug total). Each group consists of 5 male and 5 female rabbits. First dose of  
202 vaccine was delivered on Day 1 and a boost was delivered on Day 29. Body weight measurements

203 were made throughout the study. Body temperatures were measured prior to vaccination and at 6  
204 and 24 hours following vaccination on days 1 and 29. Blood collection was performed before the  
205 study and on days 1, 8, 15, 30 and 45. Urine was collected prior to the study and on days 1, 8, 15,  
206 30 and 45. Animals were sacrifice on day 45 (n = 30) for histopathological analyses from harvested  
207 tissues. Good Laboratory Practice (GLP) was followed for these experiments. Body weight and  
208 temperature were evaluated for any differences occurring during the study. Collected blood was  
209 evaluated for clinical chemistry and immunogenicity. Urinalysis was performed on collected urine  
210 samples over the course of the study. Harvested tissues underwent histopathologic evaluation for  
211 signs of toxicity.

## (A) Mouse study



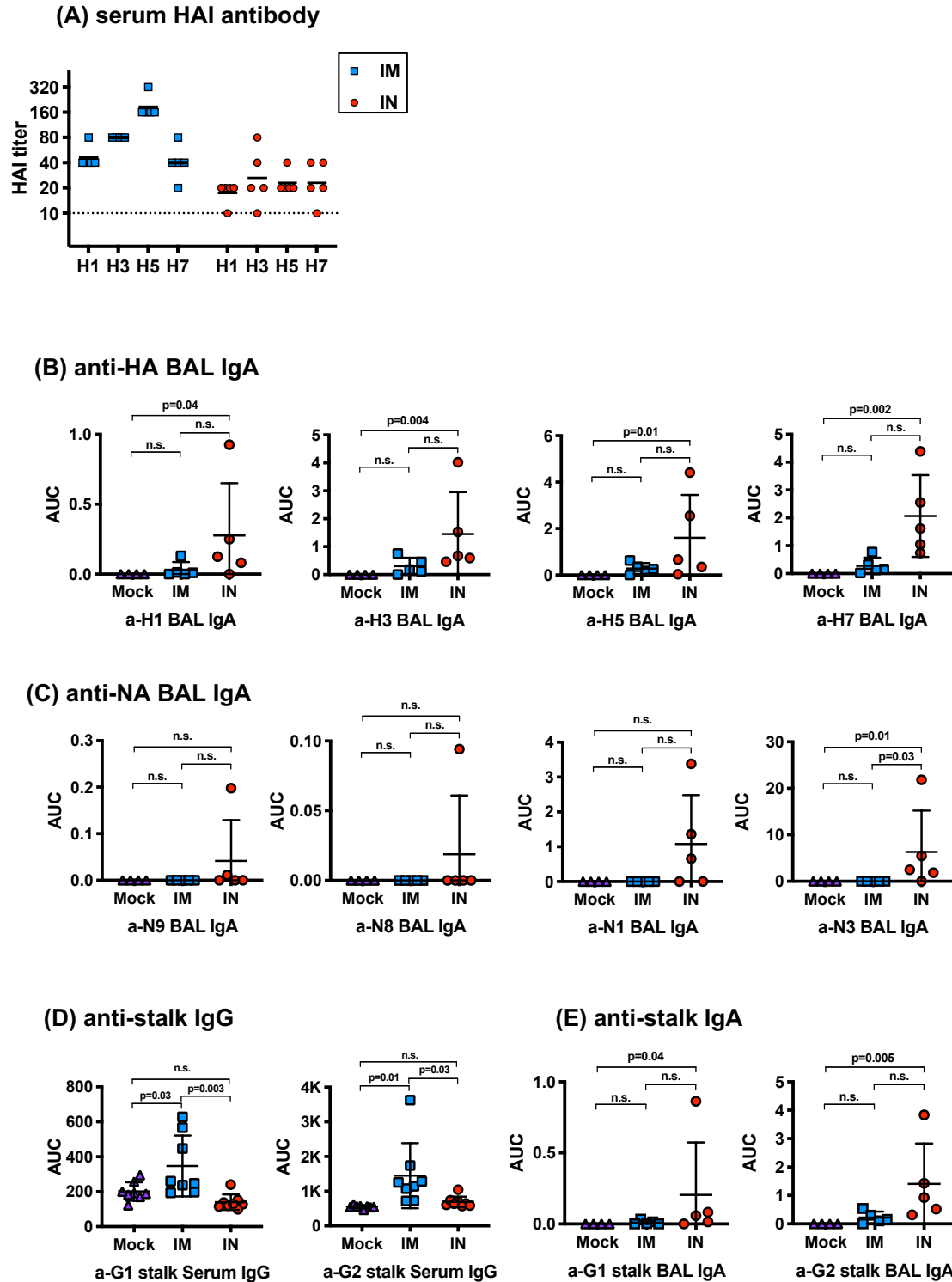
## (B) Ferret study



212

213 Fig. S1: Animal study description

214



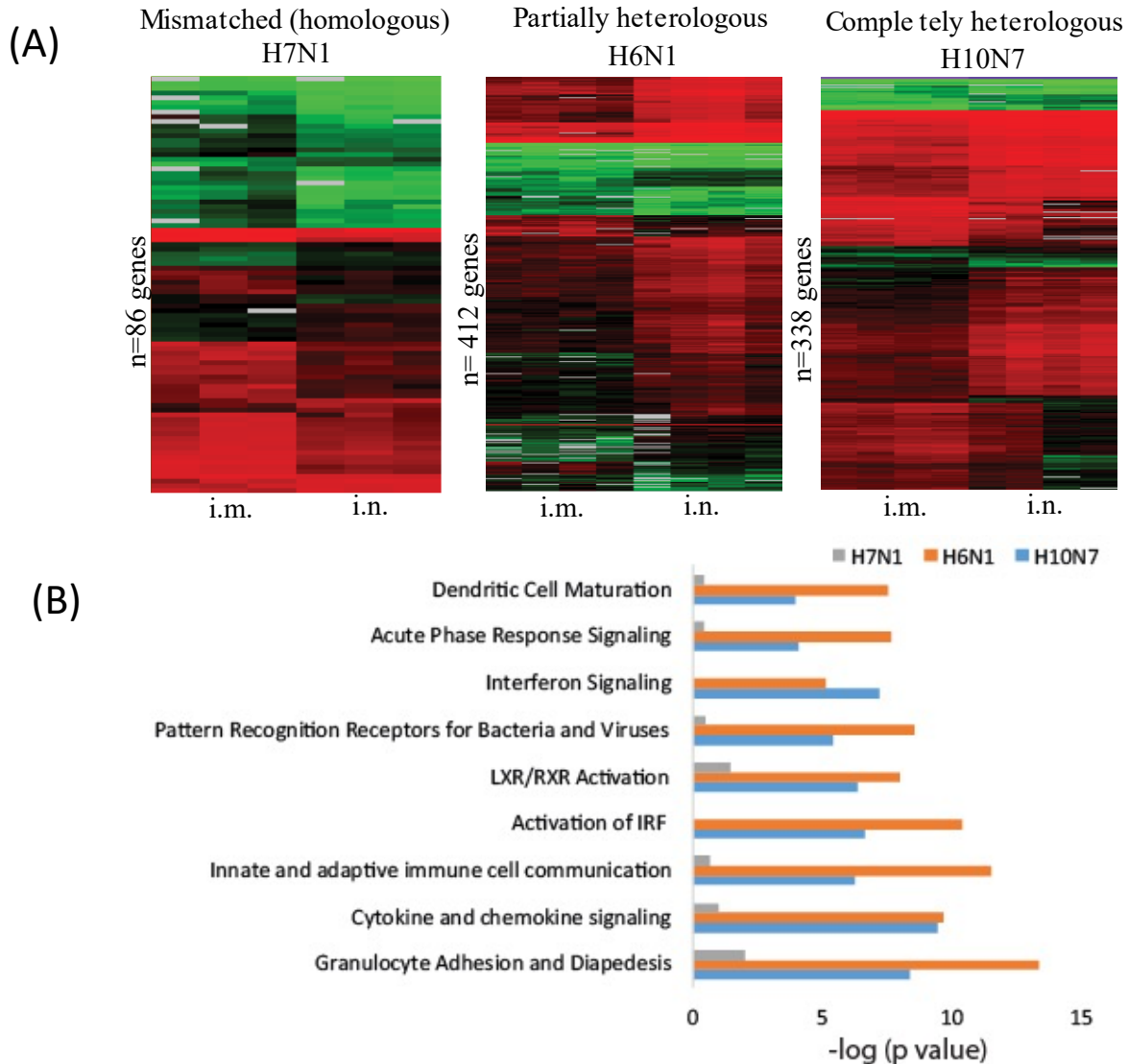
215

216 **Fig. S2: Immunogenicity in mice.** Balb/c mice were intramuscularly (IM) or intranasally (IN)

217 immunized twice with the BPL-inactivated vaccine. Serum and bronchoalveolar lavage fluid

218 (BALF) samples were collected 3-weeks-post the second immunization. **(A)** Hemagglutination  
219 inhibition (HAI) antibody titers against the four vaccine antigens were measured from serum  
220 samples from IM- or IN-vaccinated mice. The dashed line shows the detection limit of the HAI  
221 assay used. IgA levels against **(B)** four vaccine hemagglutinin (HA) antigens and **(C)** four vaccine  
222 neuraminidase (NA) antigens were measured in mock-, IM-, or IN-vaccinated mice using ELISA.  
223 **(D)** Serum IgG or **(E)** BALF IgA antibody levels against group-1 and group-2 HA stalk were  
224 measured using ELISA. Error bars represent standard deviation. Kruskal-Wallis test and post hoc  
225 Dunn's multiple comparison test were used to compare BALF IgA levels between groups.  
226 Ordinary ANOVA test and post hoc Tukey's multiple comparison test were used to compared  
227 serum IgG levels between groups. **n.s**; not significant, **AUC**; area under the curve  
228





229

230 **Supplementary Fig. S3: Differential host response to influenza infection in IN and IM**

231 **vaccinated mice.** (A) Heatmap represents transcripts showing differential expression ( $\geq 2$ -fold

232 difference in median expression level,  $p < 0.05$ ) between IN and IM vaccinated animals challenged

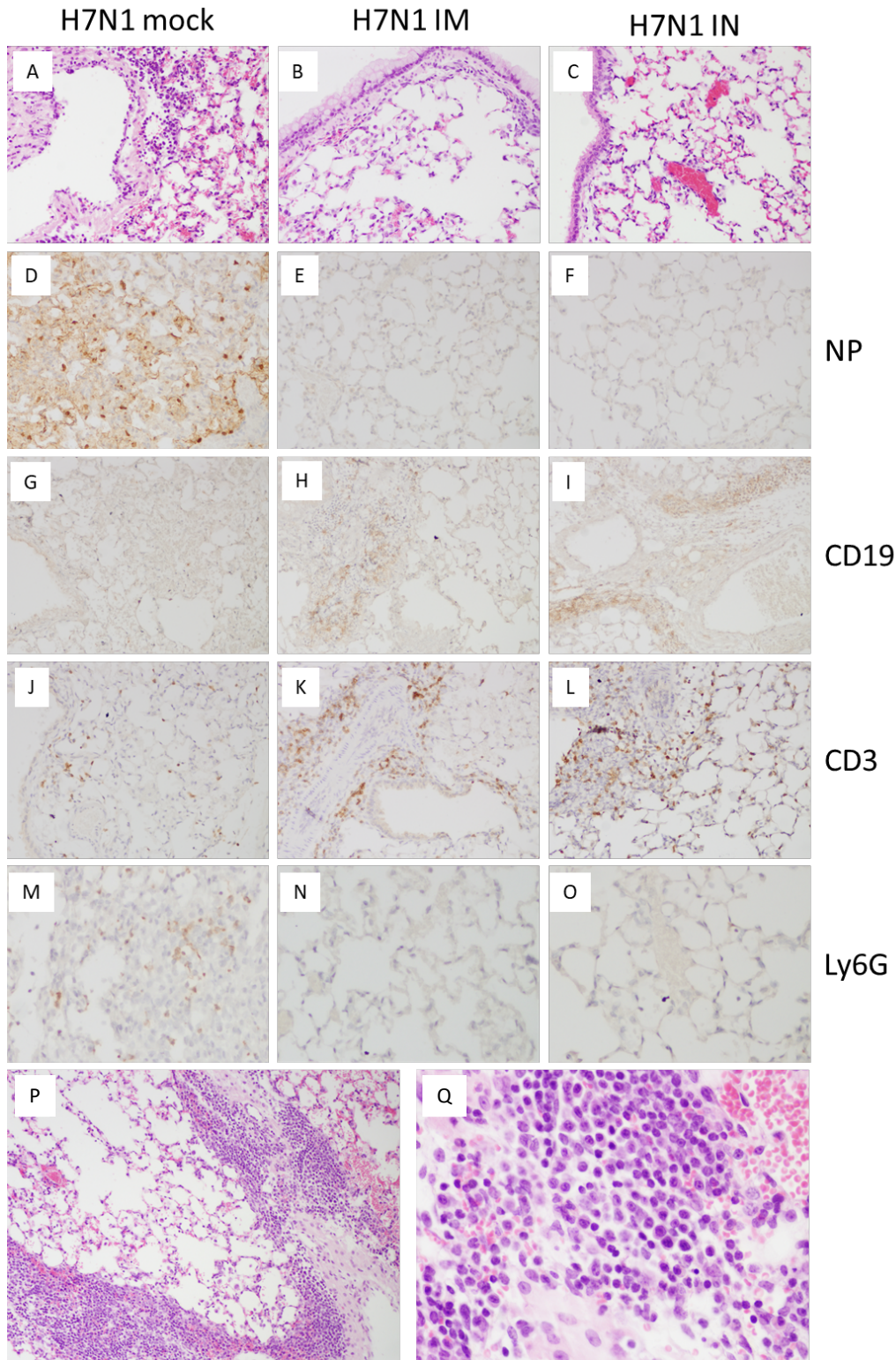
233 with either H7N1, H6N1 or H10N7 influenza virus on day 6 post-infection. Genes with increased

234 expression are show in red, genes with no change as black, and genes showing decreased

235 expression in green. (B) Gene enrichment analysis of genes showing differential expression

236 between IN and IM vaccinated animals.

237



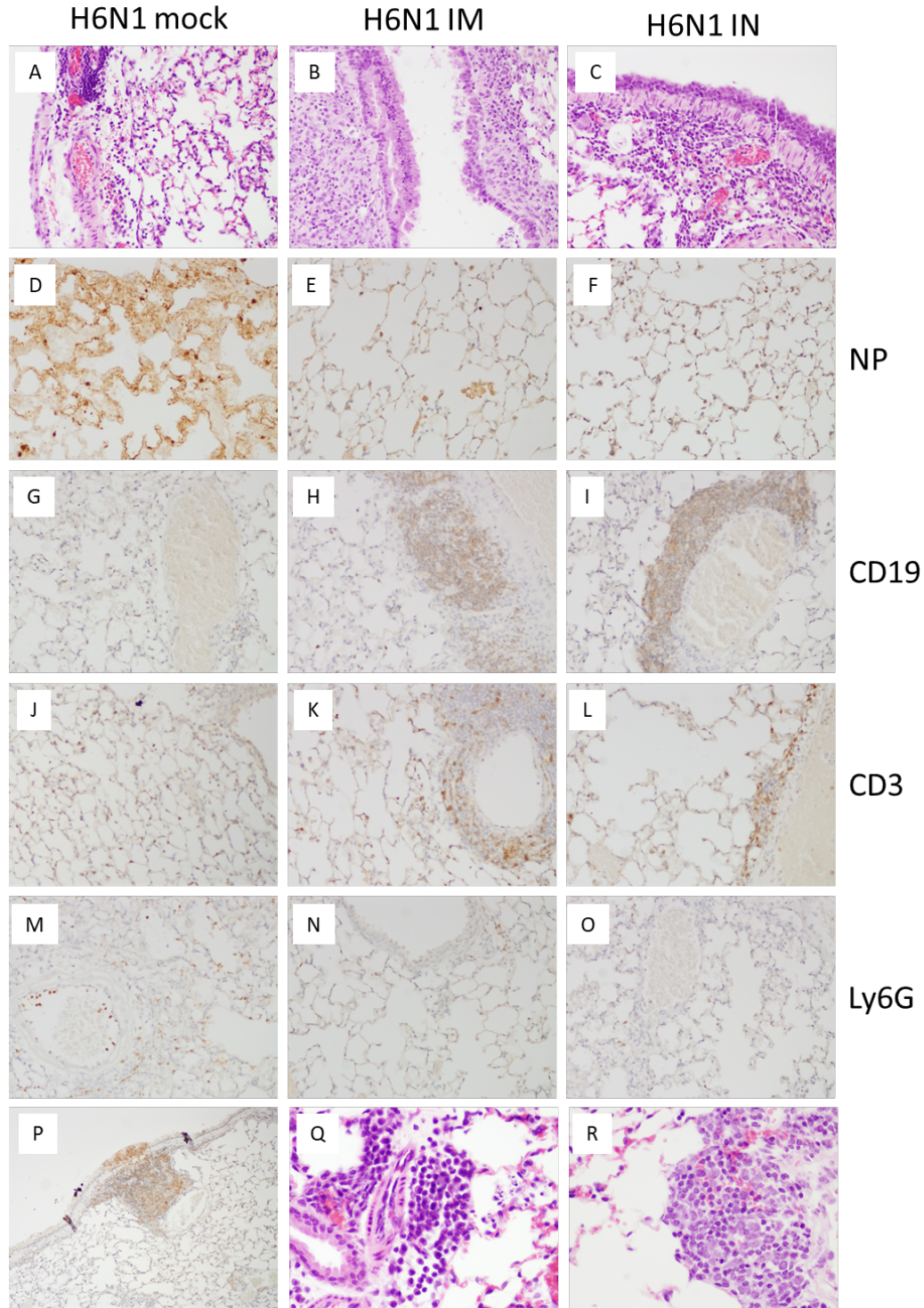
238

239 **Supplementary Fig. S4: Mouse H7N1 pathology. (A-C).** H&E stains of lung at day 5 post

240 challenge. Mock-vaccinated mice (A) challenged with the H7N1 virus showed an extensive

241 primary viral pneumonia, affecting >50% of lung with necrotizing bronchitis and bronchiolitis,  
242 and alveolitis with a neutrophil-rich inflammatory infiltrate, while IM-vaccinated mice (**B**) and  
243 IN-vaccinated mice (**C**) showed no evidence of pneumonia or inflammatory infiltrates. Original  
244 magnifications 40x. (**D-F**). Mock-vaccinated mice (**D**) challenged with the H7N1 virus showed  
245 extensive viral antigen (nucleoprotein, NP) staining in alveolar epithelial cells and alveolar  
246 macrophages, while IM-vaccinated mice (**E**) and IN-vaccinated mice (**F**) showed no viral antigen  
247 staining. Original magnifications 100x. (**G-I**). Immunostaining for CD19+ B cells. Mock-  
248 vaccinated mice (**G**) challenged with the H7N1 virus showed few, scattered CD19+ cells, while  
249 IM-vaccinated mice (**H**) and IN-vaccinated mice (**I**) showed prominent perivascular and  
250 peribronchiolar aggregates of CD19+ cells. Original magnifications 40x. (**J-L**). Immunostaining  
251 for CD3+ T cells. Mock-vaccinated mice (**J**) challenged with the H7N1 virus showed few,  
252 scattered CD3+ cells, while IM-vaccinated mice (**K**) and IN-vaccinated mice (**L**) showed  
253 prominent perivascular and peribronchiolar aggregates of CD3+ cells. Original magnifications  
254 40x. (**M-O**). Immunostaining for neutrophils with the Ly6G antibody. Mock-vaccinated mice  
255 (**M**) challenged with the H7N1 virus showed many Ly6G+ neutrophils within the lung  
256 parenchyma, while IM-vaccinated mice (**N**) and IN-vaccinated mice (**O**) showed no neutrophils.  
257 Original magnifications 100x. (**P-Q**). Large aggregates of plasma cells (staining negatively for  
258 CD19) were observed in the lungs of vaccinated animals but not in lungs of mock-vaccinated  
259 animals. Original magnifications 40 x (**P**) and 200x (**Q**).

260



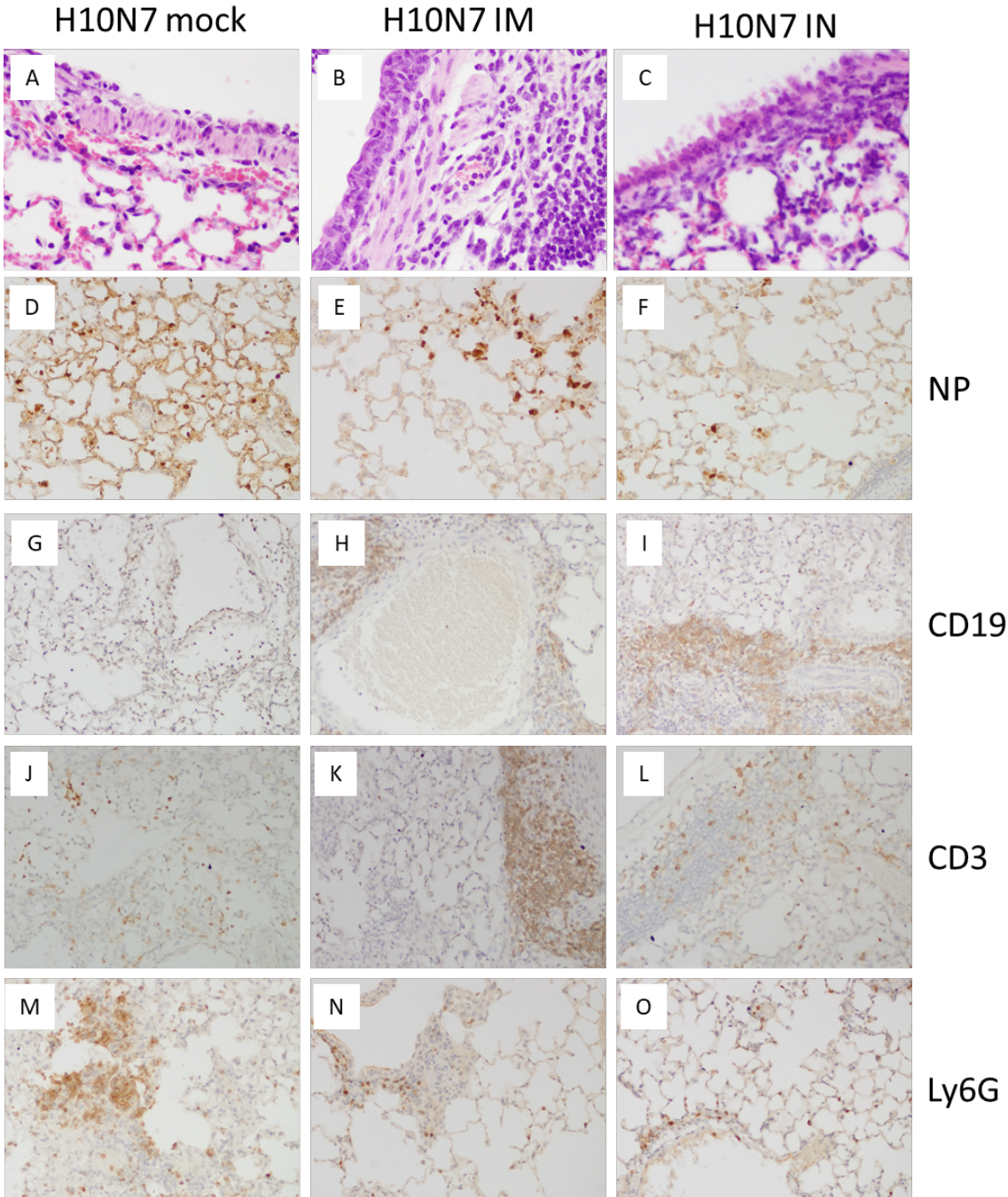
261

262 **Supplementary Fig. S5: Mouse H6N1 pathology. (A-C).** H&E stains of lung at day 5 post

263 challenge. Mock-vaccinated mice (A) challenged with the H6N1 virus showed an extensive

264 primary viral pneumonia, affecting >50% of lung with necrotizing bronchitis and bronchiolitis,

265 and alveolitis with a neutrophil-rich inflammatory infiltrate, while IM-vaccinated mice (**B**) and  
266 IN-vaccinated mice (**C**) showed little evidence of pneumonia or inflammatory infiltrates. The  
267 respiratory epithelium of vaccinated mice showed extensive re proliferation, and submucosal  
268 lymphoid aggregates were prominent. Original magnifications 40x. (**D-F**). Mock-vaccinated mice  
269 (**D**) challenged with the H7N1 virus showed extensive viral antigen (nucleoprotein, NP) staining  
270 in alveolar epithelial cells and alveolar macrophages, while IM-vaccinated mice (**E**) and IN-  
271 vaccinated mice (**F**) showed little viral antigen staining, mostly in alveolar macrophages. Original  
272 magnifications 100x. (**G-I**). Immunostaining for CD19+ B cells. Mock-vaccinated mice (**G**)  
273 challenged with the H7N1 virus showed few, scattered CD19+ cells, while IM-vaccinated mice  
274 (**H**) and IN-vaccinated mice (**I**) showed prominent perivascular and peribronchiolar aggregates of  
275 CD19+ cells. Original magnifications 40x. (**J-L**). Immunostaining for CD3+ T cells. Mock-  
276 vaccinated mice (**J**) challenged with the H7N1 virus showed few, scattered CD3+ cells, while IM-  
277 vaccinated mice (**K**) and IN-vaccinated mice (**L**) showed prominent perivascular and  
278 peribronchiolar aggregates of CD3+ cells. Original magnifications 40x. (**M-O**). Immunostaining  
279 for neutrophils with the Ly6G antibody. Mock-vaccinated mice (**M**) challenged with the H7N1  
280 virus showed many Ly6G+ neutrophils within the lung parenchyma and margination from small  
281 blood vessels, while IM-vaccinated mice (**N**) and IN-vaccinated mice (**O**) showed very few  
282 neutrophils. Original magnifications 100x. (**P-R**). IM-vaccinated animals showed small foci of  
283 intra-epithelial CD19+ B cells (**P**). Aggregates of plasma cells (staining negatively for CD19) were  
284 observed in the lungs of vaccinated animals but not in lungs of mock-vaccinated animals (**Q-R**).  
285 Original magnifications 40 x (**P**) and 200x (**Q-R**).  
286

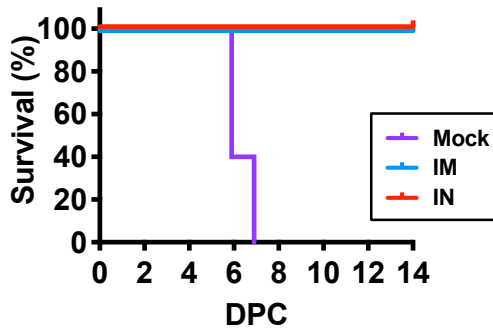


287

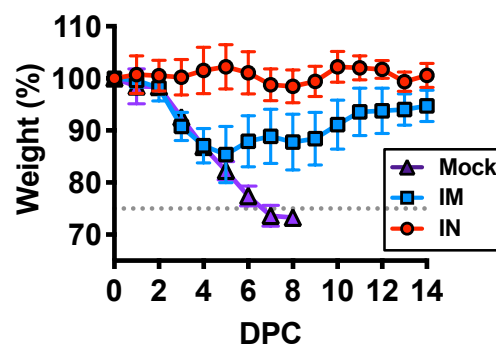
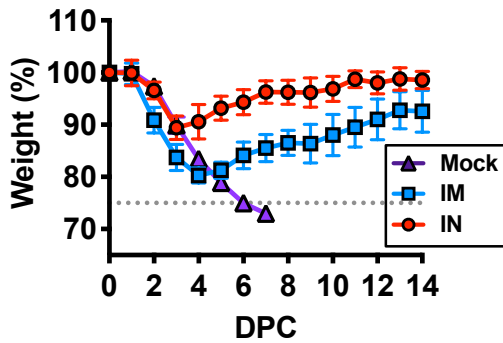
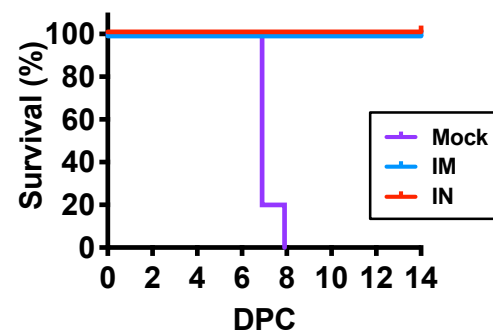
288 **Supplementary Fig. S6: Mouse H10N7 pathology. (A-C).** H&E stains of lung at day 5 post  
289 challenge. Mock-vaccinated mice (A) challenged with the H10N7 virus showed an extensive  
290 primary viral pneumonia, affecting >50% of lung with necrotizing bronchitis and bronchiolitis,  
291 and alveolitis with a neutrophil-rich inflammatory infiltrate, while IM-vaccinated mice (B) and

292 IN-vaccinated mice (**C**) showed little evidence of pneumonia or inflammatory infiltrates. The  
293 respiratory epithelium of vaccinated mice showed extensive re proliferation with prominent mitotic  
294 figures (**B**), and submucosal lymphoid aggregates were prominent. Original magnifications 40x.  
295 (**D-F**). Mock-vaccinated mice (**D**) challenged with the H7N1 virus showed extensive viral antigen  
296 (nucleoprotein, NP) staining in alveolar epithelial cells and alveolar macrophages, while IM-  
297 vaccinated mice (**E**) and IN-vaccinated mice (**F**) showed some viral antigen staining, mostly in  
298 alveolar macrophages. Original magnifications 100x. (**G-I**). Immunostaining for CD19+ B cells.  
299 Mock-vaccinated mice (**G**) challenged with the H7N1 virus showed few, scattered CD19+ cells,  
300 while IM-vaccinated mice (**H**) and IN-vaccinated mice (**I**) showed prominent perivascular and  
301 peribronchiolar aggregates of CD19+ cells. Original magnifications 40x. (**J-L**). Immunostaining  
302 for CD3+ T cells. Mock-vaccinated mice (**J**) challenged with the H7N1 virus showed few,  
303 scattered CD3+ cells, while IM-vaccinated mice (**K**) and IN-vaccinated mice (**L**) showed  
304 prominent perivascular and peribronchiolar aggregates of CD3+ cells. Original magnifications  
305 40x. (**M-O**). Immunostaining for neutrophils with the Ly6G antibody. Mock-vaccinated mice  
306 (**M**) challenged with the H7N1 virus showed large infiltrates Ly6G+ neutrophils within the lung  
307 parenchyma and margination from small blood vessels, while IM-vaccinated mice (**N**) and IN-  
308 vaccinated mice (**O**) showed only few neutrophils, mostly in peribronchiolar locations. Original  
309 magnifications 100x.  
310

**(A) H10N7 challenge - mouse**



**(B) H6N1 challenge - mouse**

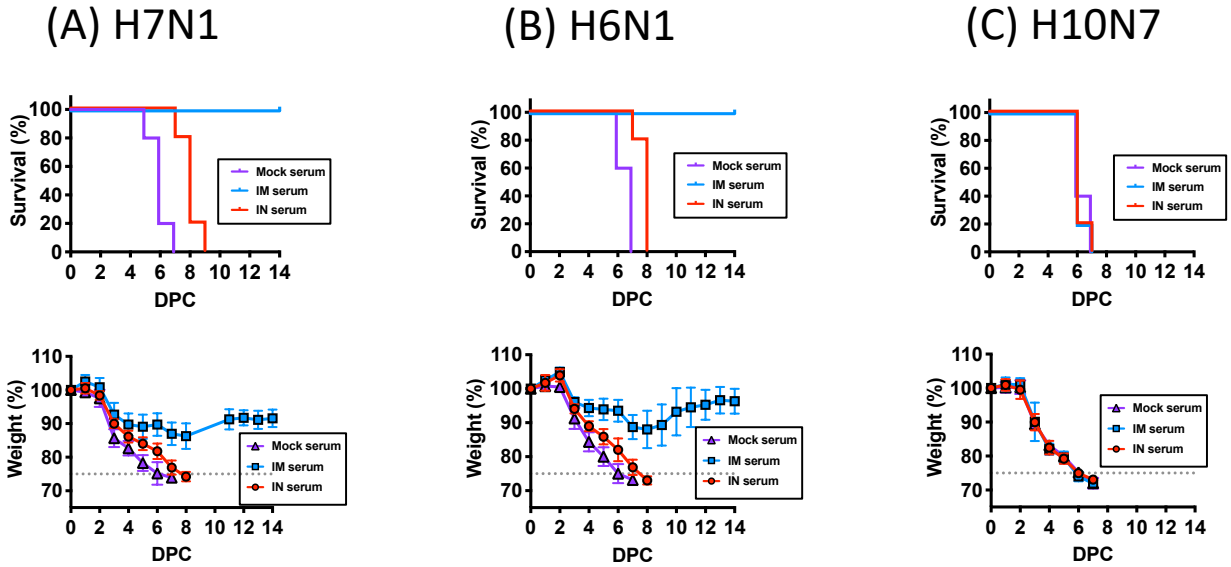


311

312 **Supplementary Fig. S7: Protection with low dose ( $1/4$ ) immunization in mice.** Balb/c mice were  
313 intramuscularly (IM) or intranasally (IN) immunized twice with the BPL-inactivated vaccine at  $1/4$   
314 dose (i.e. 1.5ug total) followed by 10x mouse 50% lethal dose (LD50) challenge. Percent survival  
315 and percent weight loss in each group (n=5) following (A) H10N7 or (B) H6N1 virus challenge  
316 are shown. Error bars represent standard deviation. **DPC**; days post-challenge

317



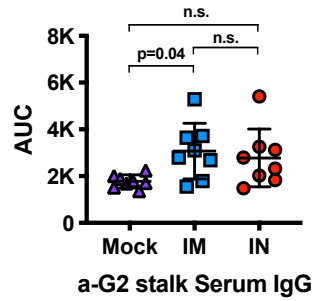
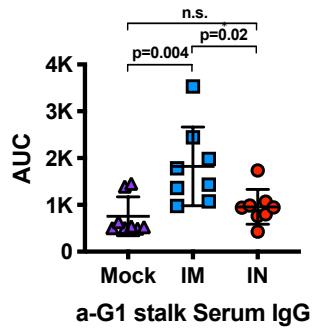


318

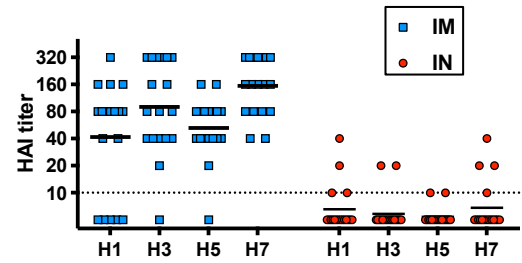
319 **Supplementary Fig. S8: Protection by passive serum transfer in mice.** Serum from mock-, IM-  
320 , or IN-vaccinated mice was injected intraperitoneally (200ul per animal) 1 day prior to 10x mouse  
321 50% lethal dose (LD50) challenge. Percent survival and percent weight loss in each group  
322 following (A) H7N1, (B) H6N1, and (C) H10N7 virus challenge are shown. Error bars represent  
323 standard deviation. **DPC**; days post-challenge

324

**(A) anti-stalk serum IgG**



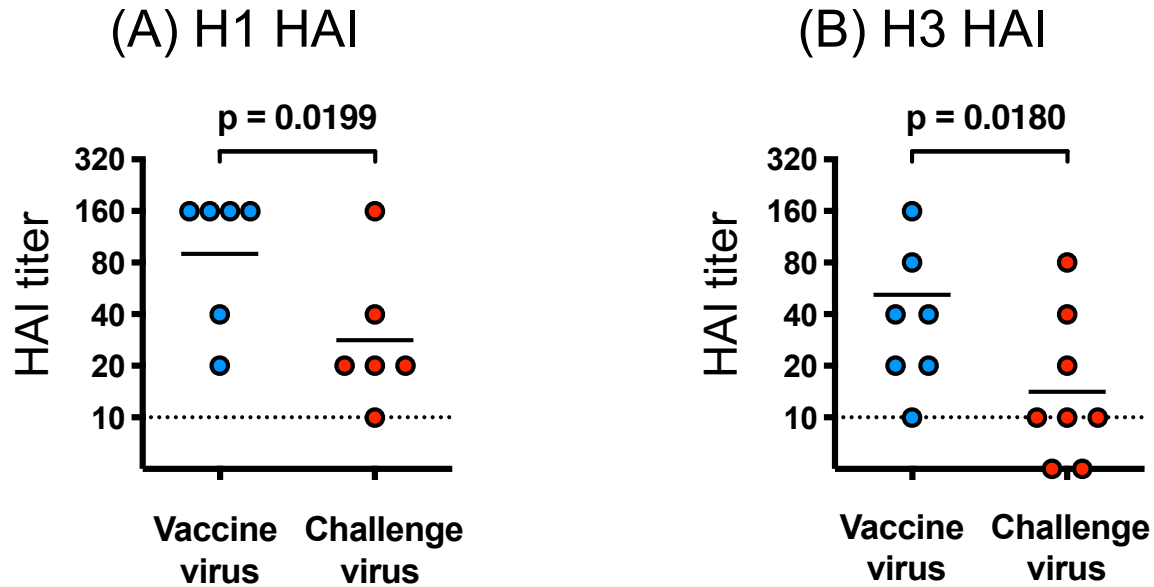
**(B) serum HAI antibody**



325

326 **Supplementary Fig. S9: Immunogenicity in ferrets.** Ferrets were intramuscularly (IM) or  
327 intranasally (IN) immunized twice with the BPL-inactivated vaccine. Serum samples were  
328 collected 3-weeks-post the second immunization. **(A)** Serum IgG levels against group-1 and  
329 group-2 HA stalk were measured by ELISA. Error bars represent standard deviation. Ordinary  
330 ANOVA test and post hoc Tukey's multiple comparison test were used to compared serum IgG  
331 levels between groups. **(B)** Hemagglutination inhibition (HAI) antibody titers against vaccine  
332 antigens were measured IM- or IN-vaccinated ferrets. The dashed line shows the detection limit  
333 of the HAI assay used. **n.s.**; not significant, **AUC**; area under the curve

334



335

336 **Supplementary Fig. S10: Antigenic differences between the vaccine strain and the challenge**

337 **strain measured by hemagglutination inhibition (HAI) assays.**

338 Ferrets were intramuscularly (IM) or intranasally (IN) immunized twice with the BPL-inactivated

339 vaccine. Serum samples were collected 3-weeks-post the second immunization. (A) Serum HAI

340 titers were measured against the vaccine strain A/mallard/Ohio/265/1987 (H1N9) and the

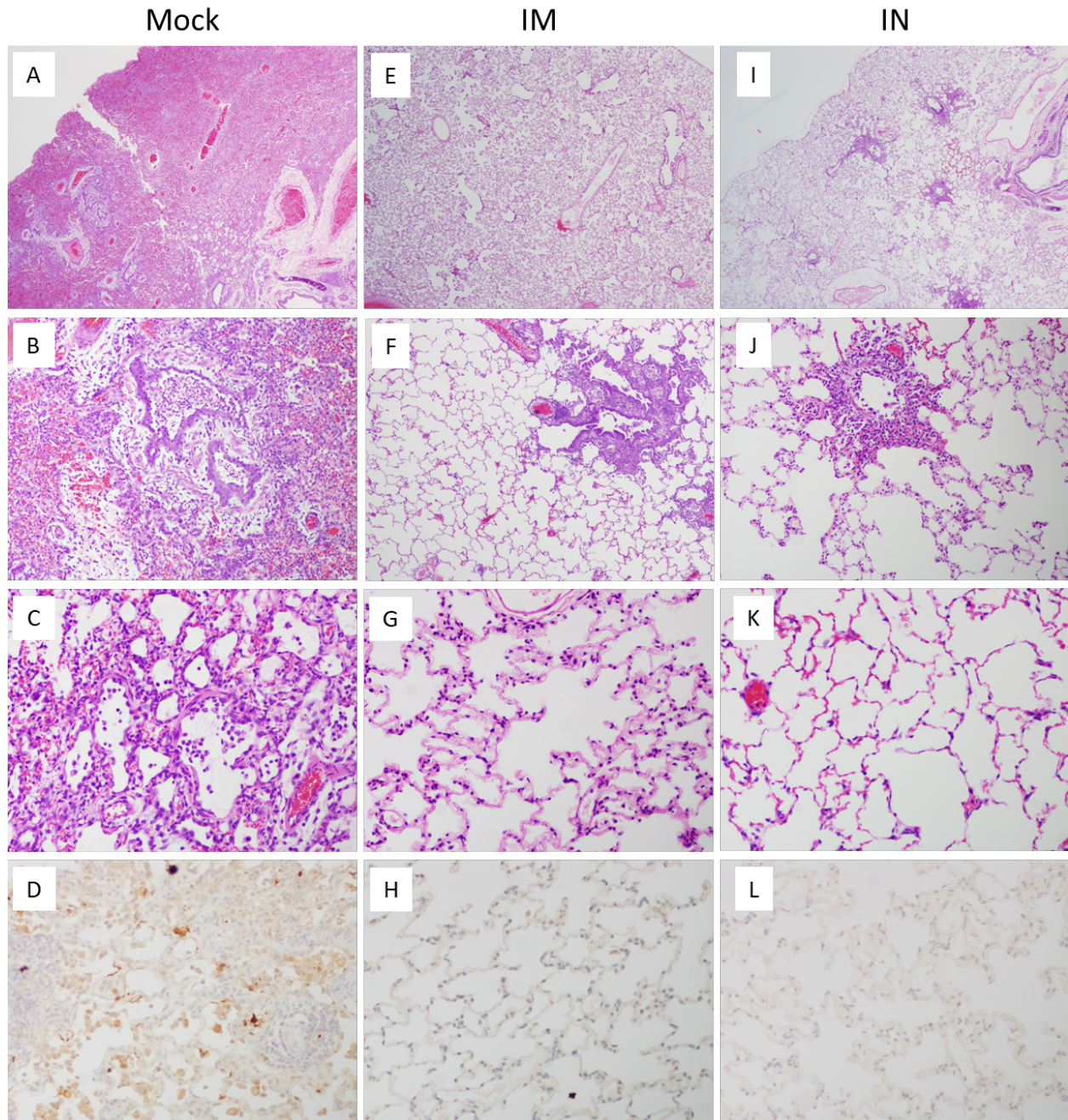
341 challenge strain A/swine/Iowa/1931 (H1N1). (B) Serum HAI titers were measured against the

342 vaccine strain A/pintail/Ohio/339/1987 (H3N8) and the challenge strain A/Port Chalmers/1973

343 (H3N2). A two-tailed paired t-test was used on log-transformed HAI titers for comparison. Bars

344 represent geometric means.

345



346

347 **Supplementary Fig. S11: Ferret H1N1 pathology. (A-C).** H&E stains of lung at day 5 post

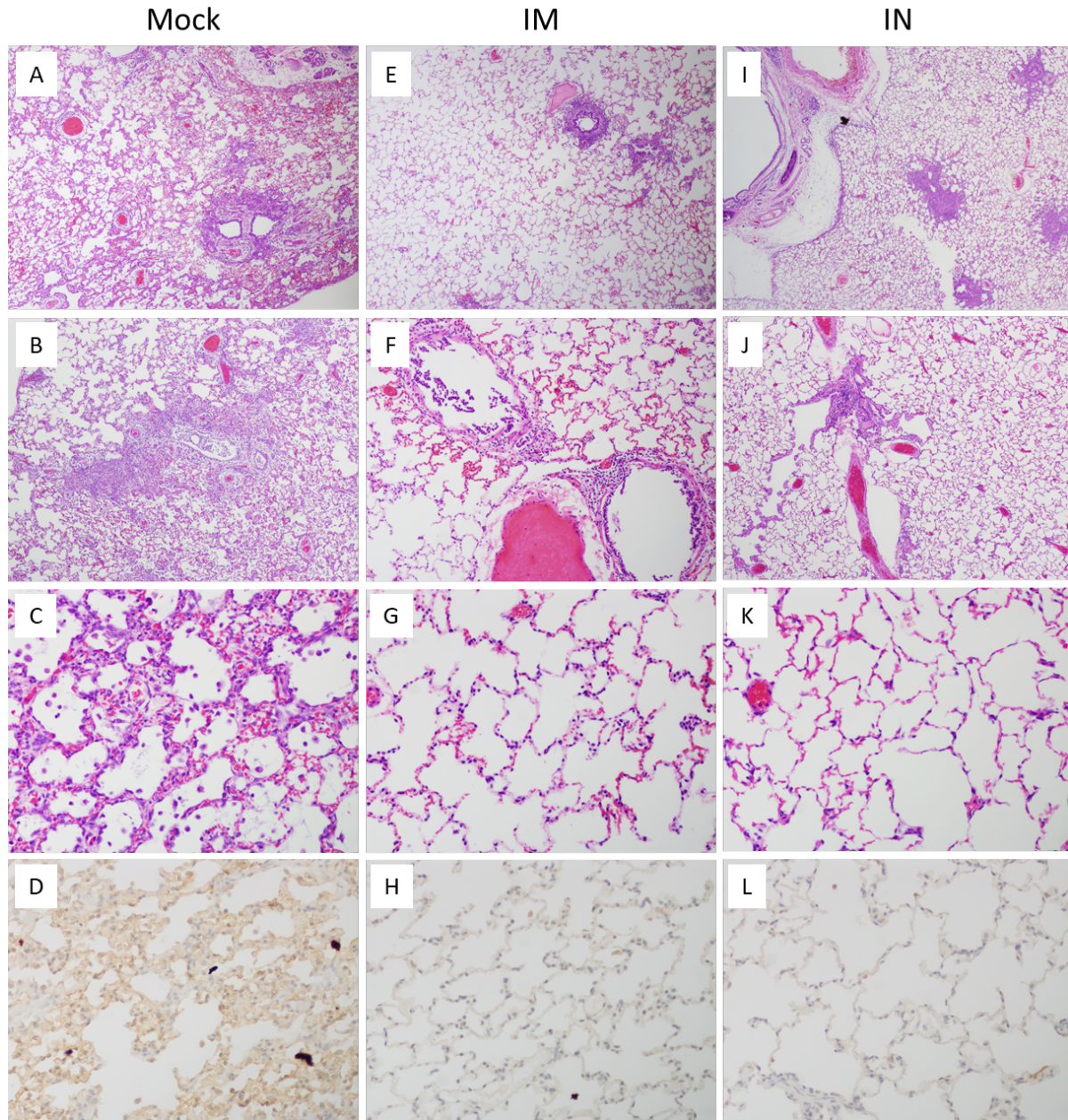
348 challenge. Mock-vaccinated ferrets (A-D) challenged with the swine/1931 H1N1 virus showed an

349 extensive primary viral pneumonia (A), affecting >50% of lung with necrotizing bronchitis and

350 bronchiolitis (B), and alveolitis with a neutrophil-rich inflammatory infiltrate (C). Immunostaining

351 revealed extensive viral antigen (nucleoprotein, NP) in alveolar epithelial cells and alveolar

352 macrophages (**D**). IM-vaccinated ferrets (**E-H**) challenged with the swine/1931 H1N1 virus  
353 showed no pneumonia (**E**), with multifocal, mild bronchiolitis (**F**), no alveolitis (**G**), and no viral  
354 antigen staining (**H**). IN-vaccinated ferrets (**I-L**) challenged with the swine/1931 H1N1 virus  
355 showed no pneumonia (**I**), with multifocal, mild bronchiolitis (**J**), no alveolitis (**K**), and no viral  
356 antigen staining (**L**). Original magnifications: 40x (**A, B, E, F, I, J**), and 100x (**C, D, G, H, K,**  
357 **L**).  
358

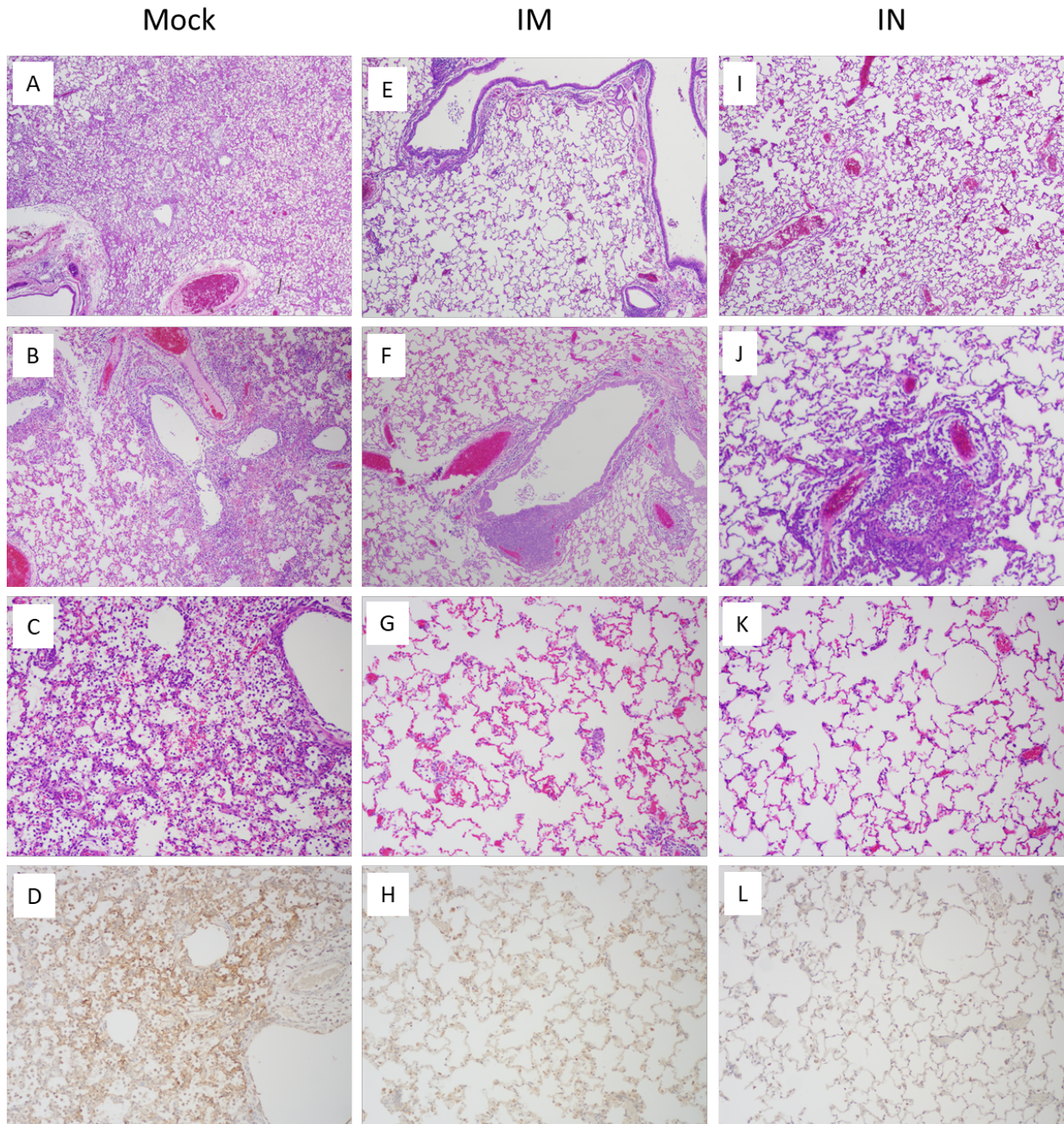


359

360 **Supplementary Fig. S12: Ferret H3N2 pathology. (A-C).** H&E stains of lung at day 5 post  
361 challenge. Mock-vaccinated ferrets (A-D) challenged with the human A/Port Chalmers/1973  
362 H3N2 virus showed an extensive primary viral pneumonia (A), affecting >50% of lung with  
363 necrotizing bronchitis and bronchiolitis (B), and alveolitis with a neutrophil-rich inflammatory  
364 infiltrate (C). Immunostaining revealed extensive viral antigen (nucleoprotein, NP) in alveolar

365 epithelial cells and alveolar macrophages (**D**). IM-vaccinated ferrets (**E-H**) challenged with the  
366 H3N2 virus showed no pneumonia (**E**), with multifocal, mild bronchiolitis (**F**), no alveolitis (**G**),  
367 and no viral antigen staining (**H**). IN-vaccinated ferrets (**I-L**) challenged with the H3N2 virus  
368 showed no pneumonia (**I**), with multifocal, mild bronchiolitis and submucosal lymphoid  
369 aggregates (**J**), no alveolitis (**K**), and no viral antigen staining (**L**). Original magnifications: 40x  
370 (**A, B, E, F, I, J**), and 100x (**C, D, G, H, K, L**).

371



372

373 **Supplementary Fig. S13: Ferret H2N7 pathology. (A-C).** H&E stains of lung at day 5 post

374 challenge. Mock-vaccinated ferrets (A-D) challenged with the chimeric H2N7 virus showed an

375 extensive primary viral pneumonia (A), affecting >50% of lung with necrotizing bronchitis and

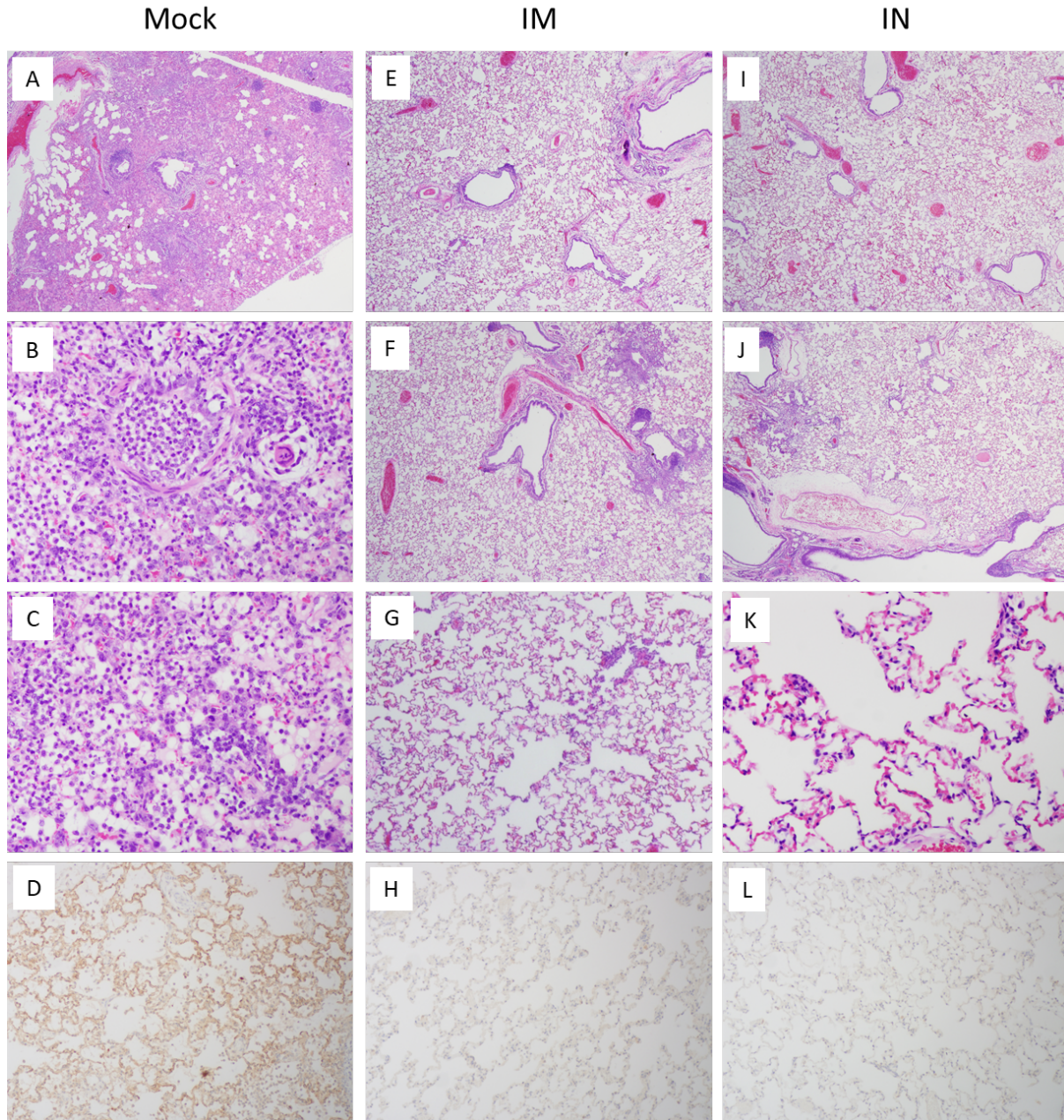
376 bronchiolitis (B), and alveolitis with a neutrophil-rich inflammatory infiltrate (C). Immunostaining

377 revealed extensive viral antigen (nucleoprotein, NP) in alveolar epithelial cells and alveolar



378 macrophages (**D**). IM-vaccinated ferrets (**E-H**) challenged with the H3N2 virus showed no  
379 pneumonia (**E**), with multifocal, mild bronchiolitis with prominent submucosal lymphoid  
380 aggregates (**F**), no alveolitis (**G**), and no viral antigen staining (**H**). IN-vaccinated ferrets (**I-L**)  
381 challenged with the H3N2 virus showed no pneumonia (**I**), with multifocal, mild bronchiolitis and  
382 submucosal lymphoid aggregates (**J**), no alveolitis (**K**), and no viral antigen staining (**L**). Original  
383 magnifications: 40x (**A, B, E, F, I, J**), and 100x (**C, D, G, H, K, L**).

384



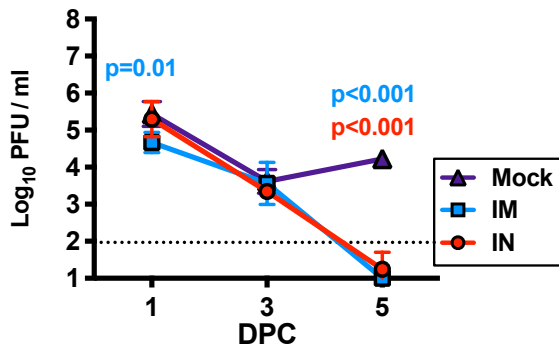
385

386 **Supplementary Fig. S14: Ferret H10N7 pathology. (A-C).** H&E stains of lung at day 5 post  
387 challenge. Mock-vaccinated ferrets (A-D) challenged with the chimeric H10N7 virus showed an  
388 extensive primary viral pneumonia (A), affecting >50% of lung with necrotizing bronchitis and  
389 bronchiolitis (B), and alveolitis with a neutrophil-rich inflammatory infiltrate (C). Immunostaining  
390 revealed extensive viral antigen (nucleoprotein, NP) in alveolar epithelial cells and alveolar

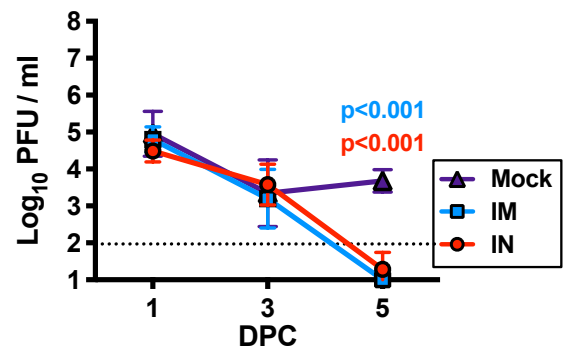
391 macrophages (**D**). IM-vaccinated ferrets (**E-H**) challenged with the H3N2 virus showed no  
392 pneumonia (**E**), with multifocal, mild bronchiolitis with prominent submucosal lymphoid  
393 aggregates (**F**), no alveolitis (**G**), and no viral antigen staining (**H**). IN-vaccinated ferrets (**I-L**)  
394 challenged with the H3N2 virus showed no pneumonia (**I**), with multifocal, mild bronchiolitis and  
395 submucosal lymphoid aggregates (**J**), no alveolitis (**K**), and no viral antigen staining (**L**). Original  
396 magnifications: 40x (**A, B, E, F, I, J**), and 100x (**C, D, G, H, K, L**).

397

(A) H1N1 challenge - ferret



(B) H3N2 challenge - ferret



398

399 **Supplementary Fig. S15: Protection with low dose (1/4) immunization in ferrets.** Ferrets were

400 intramuscularly (IM) or intranasally (IN) immunized twice with the BPL-inactivated vaccine at 1/4

401 dose (i.e.100ug total) and challenged with (A) A/swine/Iowa/1931 (H1N1) virus or (B) A/Port

402 Chalmers/1973 (H3N2) virus. Nasal wash samples were collected at days 1, 3, and 5, and the titer

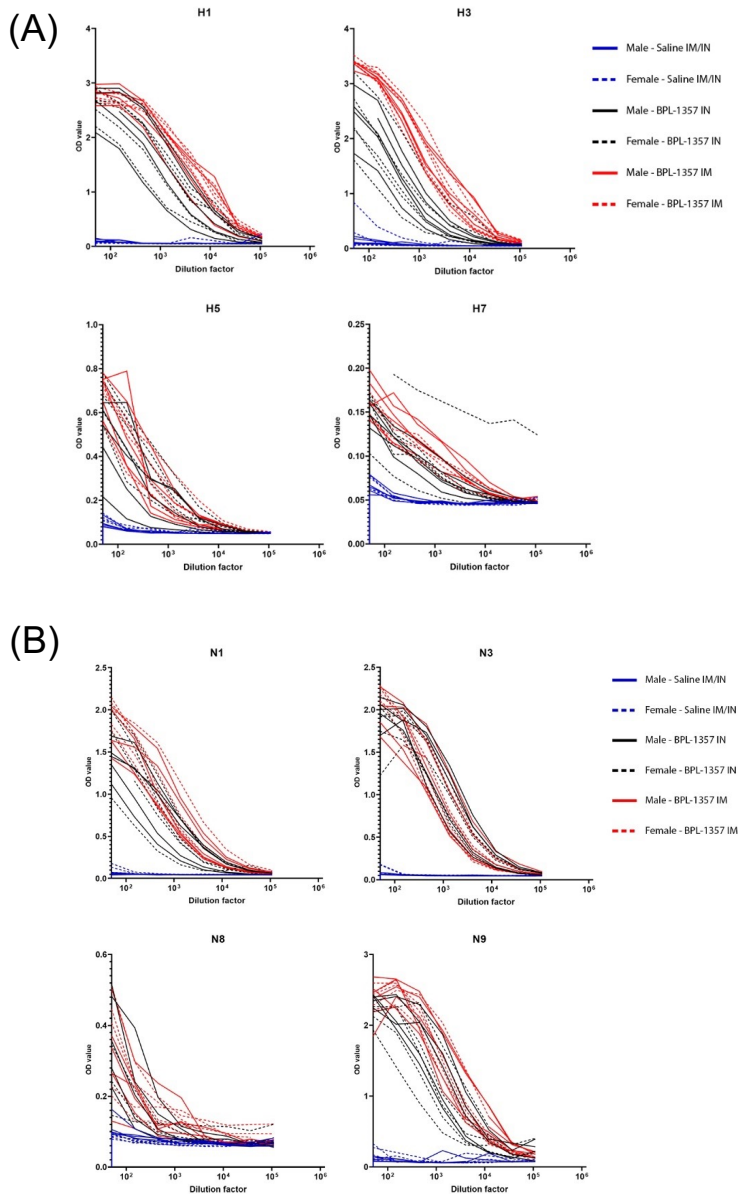
403 was measured using plaque assay. Ordinary ANOVA test and post hoc Dunnett's multiple

404 comparison test were used to compare viral titers in IM- or IN-vaccinated ferrets to mock-

405 vaccinated ferrets. Error bars represent geometric standard deviation. Dashed lines show the

406 detection limit of the plaque assay used. **DPC**; days post-challenge

407



408

409 **Supplementary Fig. S16: Immunogenicity of the vaccine in New Zealand white rabbits.** Good

410 Manufacturing Practice (GMP) manufacturing of the multivalent BPL-inactivated vaccine was

411 performed in certified Vero cells. Immunogenicity of the GMP-manufactured vaccine was tested

412 in thirty New Zealand White Rabbits following two immunizations 4 weeks apart. Ten rabbits

413 were intranasally (IN) immunized with the GMP vaccine (n=10; 5 male, 5 female). Ten rabbits

414 were intramuscularly (IM) immunized with the GMP vaccine (n=10; 5 male, 5 female). Ten

415 control rabbits received saline administered by IN (240  $\mu$ L; 120  $\mu$ L per naris) and IM (n = 10; 5  
416 male & 5 female). Serum samples were collected 16-days-post the second immunization, and the  
417 serum IgG levels against **(A)** four vaccine hemagglutinin (HA) antigens and **(B)** four vaccine  
418 neuraminidase (NA) antigens were measured using ELISA.  
419

420 **Supplementary Table S1. Vaccine strains**

<b>Vaccine Strains</b>	<b>Hemagglutinin (HA) GenBank accession number</b>	<b>Neuraminidase (NA) GenBank accession number</b>
<i>A/mallard/Ohio/265/1987 (H1N9)</i>	CY017275	CY017277
<i>A/pintail/Ohio/339/1987 (H3N8)</i>	CY019197	CY019199
<i>A/mallard/Maryland/802/2007 (H5N1)</i>	CY053877	CY053879
<i>A/environment/Maryland/261/2006 (H7N3)</i>	CY022749	CY022751

421

422

423 **Supplementary Table S2. Challenge virus HA and NA identity to vaccine virus components**

<b>Mouse Challenge Influenza A viruses (10xLD<sub>50</sub>) and Identity to Vaccine Viruses</b>		
Subtype (strain)	Percent nucleotide (and amino acid) identities	
	HA	NA
H1N1 (A/Brevig Mission/1/1918)	79.1% (92.8%)	85.5% (91.5%)
H5N8 (A/chicken/Netherlands/EMC-3/2014)	79.7% (85.6%)	76.8% (84.8%)
H6N1 (recombinant Avian) <sup>§</sup>	51.0% (63.1%) [vs H1]*	92.1% (96.2%)
H7N1 (recombinant Avian) <sup>§</sup>	100.0% (100%)	92.1% (96.2)
H7N9 (A/Shanghai/1/2013)	76.9% (84.8%)	91.0% (95.5%)
H10N7 (recombinant Avian) <sup>§</sup>	48.5% (65.8%) [vs H7]*	53.9% (58.7%) [vs N9]*

<b>Ferret Challenge Influenza A viruses (10xLD<sub>50</sub>) and Identity to Vaccine Viruses</b>		
Subtype (strain)	Percent nucleotide (and amino acid) identities	
	HA	NA
H1N1 (A/swine/Iowa/1931)	77.6% (89.9%)	85.5% (89.8%)
H2N7 (recombinant with 1957 Pandemic HA) <sup>§</sup>	44.9% (42.5%) [vs H1]*	53.9% (58.7) [vs N9]*
H3N2 (A/Port Chalmers/1973)	83.8% (94.2%)	43.5% (50.4) [vs N3]*
H10N7 (recombinant Avian) <sup>§</sup>	48.5% (65.8%) [vs H7]*	53.9% (58.7) [vs N9]*

424

425 §Recombinant avian influenza A viruses made as 2:6 recombinants with above HA and NA gene segments with  
 426 remaining 6 gene segments from A/green winged teal/Ohio/175/1986 (H2N1) [ref Qi].

427 \*Heterosubtypic HA and/or NA challenge virus homologies were compared to phylogenetically closest vaccine  
 428 sequence as noted.

429



## 430 References

- 431 1. L. Qi *et al.*, Role of sialic acid binding specificity of the 1918 influenza virus  
432 hemagglutinin protein in virulence and pathogenesis for mice. *J Virol* **83**, 3754-3761  
433 (2009).
- 434 2. T. M. Tumpey *et al.*, Characterization of the reconstructed 1918 Spanish influenza  
435 pandemic virus. *Science* **310**, 77-80 (2005).
- 436 3. L. Qi *et al.*, Contemporary avian influenza A virus subtype H1, H6, H7, H10, and H15  
437 hemagglutinin genes encode a mammalian virulence factor similar to the 1918  
438 pandemic virus H1 hemagglutinin. *mBio* **5**, e02116 (2014).
- 439 4. B. Reynes, E. M. van Schothorst, J. Keijer, A. Palou, P. Oliver, Effects of cold exposure  
440 revealed by global transcriptomic analysis in ferret peripheral blood mononuclear cells.  
441 *Sci Rep* **9**, 19985 (2019).
- 442 5. J. A. Runstadler *et al.*, Using RRT-PCR analysis and virus isolation to determine the  
443 prevalence of avian influenza virus infections in ducks at Minto Flats State Game Refuge,  
444 Alaska, during August 2005. *Arch Virol* **152**, 1901-1910 (2007).
- 445 6. E. Spackman *et al.*, Development of a real-time reverse transcriptase PCR assay for type  
446 A influenza virus and the avian H5 and H7 hemagglutinin subtypes. *J Clin Microbiol* **40**,  
447 3256-3260 (2002).
- 448 7. L. J. Reed, M. H., A simple method of estimating fifty percent endpoints. *Am. J.*  
449 *Epidemiol* **27**, 493-497 (1938).
- 450 8. Manual for the laboratory diagnosis and virological surveillance of influenza. World  
451 Health Organization. ISBN 978 9241548090:43-62:  
452 [http://whqlibdoc.who.int/publications/2011/9789241548090\\_eng.pdf](http://whqlibdoc.who.int/publications/2011/9789241548090_eng.pdf)., (2011).
- 453 9. F. Krammer *et al.*, A carboxy-terminal trimerization domain stabilizes conformational  
454 epitopes on the stalk domain of soluble recombinant hemagglutinin substrates. *PLoS*  
455 *One* **7**, e43603 (2012).
- 456 10. X. Xu, X. Zhu, R. A. Dwek, J. Stevens, I. A. Wilson, Structural characterization of the 1918  
457 influenza virus H1N1 neuraminidase. *J Virol* **82**, 10493-10501 (2008).
- 458 11. J. K. Park *et al.*, Evaluation of Preexisting Anti-Hemagglutinin Stalk Antibody as a  
459 Correlate of Protection in a Healthy Volunteer Challenge with Influenza A/H1N1pdm  
460 Virus. *MBio* **9**, (2018).
- 461 12. F. Krammer, N. Pica, R. Hai, I. Margine, P. Palese, Chimeric hemagglutinin influenza virus  
462 vaccine constructs elicit broadly protective stalk-specific antibodies. *J Virol* **87**, 6542-  
463 6550 (2013).
- 464 13. L. Qi *et al.*, Analysis by single-gene reassortment demonstrates that the 1918 influenza  
465 virus is functionally compatible with a low-pathogenicity avian influenza virus in mice. *J*  
466 *Virol* **86**, 9211-9220 (2012).
- 467